
Visual-Inertial-Wheel Odometry with Online Calibration

Woosik Lee - woosik@udel.edu
Kevin Ekenhoff - keck@udel.edu
Yulin Yang - yuyang@udel.edu
Patrick Geneva - pgeneva@udel.edu
Chuchu Chen - ccchu@udel.edu
Guoquan Huang - ghuang@udel.edu

Department of Mechanical Engineering
University of Delaware, Delaware, USA

RPNG

Robot Perception and Navigation Group (RPNG)
Tech Report - RPNG-2020-VIWO
Last Updated - November 3, 2021

Contents

1	VIO with MSCKF	1
1.1	The State Vector	1
1.2	IMU State Propagation	1
1.3	Visual Measurement Update	2
2	Wheel-Encoder Measurement Model	4
2.1	Wheel Odometry Preintegration	4
2.2	Odometry Measurement wrt. Intrinsic	6
2.3	Odometry Measurement wrt. Extrinsic	9
	2.3.1 Spatial calibration	9
	2.3.2 Temporal calibration	11
2.4	Odometry Measurement Update	12
3	Observability Analysis	13
3.1	State Transition Matrix	13
3.2	Observability Properties	15
	References	21

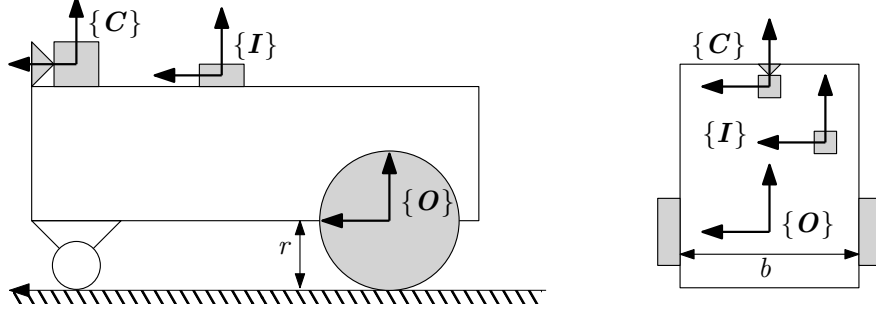


Figure 1: Frames used in this report

1 VIO with MSCKF

1.1 The State Vector

In this technical report, we analyze a robot that carries Inertial Measurement Unit (**IMU**), visual sensor (**camera**), and two separately driven **wheel sensors**. First, we briefly review the visual-inertial odometry (VIO) within the standard MSCKF framework [1], which serve as the baseline for the proposed visual-inertial-wheel odometry (VIWO) system.

Specifically, at time t_k , the state vector \mathbf{x}_k consists of the current inertial state \mathbf{x}_{I_k} and n historical IMU pose clones \mathbf{x}_{C_k} represented in the global frame $\{G\}$:

$$\mathbf{x}_k = [\mathbf{x}_{I_k}^\top \quad \mathbf{x}_{C_k}^\top]^\top \quad (1)$$

$$\mathbf{x}_{I_k} = \left[\begin{matrix} I_k \bar{q}^\top & G \mathbf{p}_{I_k}^\top & G \mathbf{v}_{I_k}^\top & \mathbf{b}_g^\top & \mathbf{b}_a^\top \end{matrix} \right]^\top \quad (2)$$

$$\mathbf{x}_{C_k} = \left[\begin{matrix} I_{k-1} \bar{q}^\top & G \mathbf{p}_{I_{k-1}}^\top & \cdots & I_{k-n} \bar{q}^\top & G \mathbf{p}_{I_{k-n}}^\top \end{matrix} \right]^\top \quad (3)$$

where $I_k \bar{q}$ is the JPL unit quaternion [2] corresponding to the rotation $I_k \mathbf{R}$ from $\{G\}$ to IMU frame $\{I\}$, $G \mathbf{p}_{I_k}$ and $G \mathbf{v}_{I_k}$ are the position and velocity of $\{I\}$ in $\{G\}$, and \mathbf{b}_g and \mathbf{b}_a are the biases of the gyroscope and accelerometer. We define $\mathbf{x} = \hat{\mathbf{x}} \boxplus \tilde{\mathbf{x}}$, where \mathbf{x} is the true state, $\hat{\mathbf{x}}$ is its estimate, $\tilde{\mathbf{x}}$ is the error state, and the operation \boxplus which maps the error state vector to its corresponding manifold [3].

By using Extended Kalman Filter, we propagate the state with IMU measurements and update the state with visual and wheel measurements. The IMU propagation and the visual sensor update is not the main scope of this paper, so will be briefly described within the following chapters.

1.2 IMU State Propagation

The angular velocity $\boldsymbol{\omega}_m$ and linear acceleration \mathbf{a}_m measurements of the IMU are used for inertial state \mathbf{x}_I propagation:

$$\boldsymbol{\omega}_m = \boldsymbol{\omega} + \mathbf{b}_g + \mathbf{n}_g \quad (4)$$

$$\mathbf{a}_m = \mathbf{a} + I_G \mathbf{R} \mathbf{g} + \mathbf{b}_a + \mathbf{n}_a \quad (5)$$

where \mathbf{a} and $\boldsymbol{\omega}$ are true acceleration and angular velocity, \mathbf{b}_g and \mathbf{b}_a are biases of gyroscope and accelerometer, $\mathbf{g} \approx [0 \ 0 \ 9.81]^\top$ is the global gravity, and \mathbf{n}_a and \mathbf{n}_g are zero mean Gaussian noises. These measurements are used to propagate the inertial state from timestep k to $k+1$ based on the

following generic nonlinear kinematic model [2]:

$$\hat{\mathbf{x}}_{I_{k+1|k}} = f(\hat{\mathbf{x}}_{I_{k|k}}, \mathbf{a}_{m_k}, \boldsymbol{\omega}_{m_k}) \quad (6)$$

where $\hat{\mathbf{x}}_{I_{a|b}}$ denotes the estimate at timestep a processing the measurements up to timestep b . In order to propagate the corresponding covariance matrix, we use the *error state transition matrix* $\Phi_I(t_{k+1}, t_k)$ and the Jaconian matrix of $f(\cdot)$ respect to the noise \mathbf{G}_k as:

$$\mathbf{P}_{I_{k+1|k}} = \Phi_I(t_{k+1}, t_k) \mathbf{P}_{I_{k|k}} \Phi_I(t_{k+1}, t_k)^\top + \mathbf{G}_k \mathbf{Q}_d \mathbf{G}_k^\top \quad (7)$$

where $[\mathbf{n}_g^\top, \mathbf{n}_a^\top, \mathbf{n}_{\omega g}^\top, \mathbf{n}_{\omega a}^\top]^\top \sim \mathcal{N}(\mathbf{0}, \mathbf{Q}_d)$, and $\mathbf{n}_{\omega g}$ and $\mathbf{n}_{\omega a}$ are white Gaussian noises of gyroscope and accelerometer bias random walk model. In this report, we refer to [4] for the matrix $\Phi_I(t_{k+1}, t_k)$, which is:

$$\Phi_I(t_{k+1}, t_k) = \begin{bmatrix} \Phi_{I_{11}}(t_{k+1}, t_k) & \mathbf{0}_3 & \mathbf{0}_3 & \Phi_{I_{14}}(t_{k+1}, t_k) & \mathbf{0}_3 \\ \Phi_{I_{21}}(t_{k+1}, t_k) & \mathbf{I}_3 & \Phi_{I_{23}}(t_{k+1}, t_k) & \Phi_{I_{24}}(t_{k+1}, t_k) & \Phi_{I_{25}}(t_{k+1}, t_k) \\ \Phi_{I_{31}}(t_{k+1}, t_k) & \mathbf{0}_3 & \mathbf{I}_3 & \Phi_{I_{34}}(t_{k+1}, t_k) & \Phi_{I_{35}}(t_{k+1}, t_k) \\ \mathbf{0}_3 & \mathbf{0}_3 & \mathbf{0}_3 & \mathbf{I}_3 & \mathbf{0}_3 \\ \mathbf{0}_3 & \mathbf{0}_3 & \mathbf{0}_3 & \mathbf{0}_3 & \mathbf{I}_3 \end{bmatrix} \quad (8)$$

$$\Phi_{I_{11}}(t_{k+1}, t_k) = \hat{\mathbf{R}}_{I_k}^{I_{k+1}} \quad \Phi_{I_{14}}(t_{k+1}, t_k) = - \int_{t_k}^{t_{k+1}} I_{I_k}^\tau \hat{\mathbf{R}}^\top d\tau \quad (9)$$

$$\Phi_{I_{21}}(t_{k+1}, t_k) = [{}^G \hat{\mathbf{p}}_{I_k} + {}^G \hat{\mathbf{v}}_{I_k} \Delta t - {}^G \hat{\mathbf{p}}_{I_{k+1}} - \frac{1}{2} {}^G \mathbf{g} \Delta t^2]_{I_k} \hat{\mathbf{R}}^\top \quad \Phi_{I_{23}}(t_{k+1}, t_k) = \Delta t \mathbf{I}_3 \quad (10)$$

$$\Phi_{I_{24}}(t_{k+1}, t_k) = \int_{t_k}^{\theta} \int_{t_k}^{t_{k+1}} I_s \hat{\mathbf{R}}^\top [I_s \mathbf{a}] \int_{t_k}^s I_\tau \hat{\mathbf{R}}^\top d\tau ds d\theta \quad \Phi_{I_{25}}(t_{k+1}, t_k) = - \int_{t_k}^{t_{k+1}} \int_{t_k}^s I_\tau \hat{\mathbf{R}}^\top d\tau ds \quad (11)$$

$$\Phi_{I_{31}}(t_{k+1}, t_k) = [{}^G \hat{\mathbf{v}}_{I_k} - {}^G \hat{\mathbf{v}}_{I_{k+1}} - {}^G \mathbf{g} \Delta t]_{I_k} \hat{\mathbf{R}}^\top \quad \Phi_{I_{34}}(t_{k+1}, t_k) = \int_{t_k}^{t_{k+1}} I_s \hat{\mathbf{R}}^\top [I_s \mathbf{a}] \int_{t_k}^s I_\tau \hat{\mathbf{R}}^\top d\tau ds \quad (12)$$

$$\Phi_{I_{35}}(t_{k+1}, t_k) = \int_{t_k}^{t_{k+1}} I_\tau \hat{\mathbf{R}}^\top d\tau \quad (13)$$

where $[\cdot]$ is the skew-symmetric matrix and $\Delta t = t_{k+1} - t_k$.

Note that we only showed the error transition matrix for inertial state, not for whole state, which will be handled in later chapter 3.

1.3 Visual Measurement Update

We maintain a number of stochastic clones in \mathbf{x}_{C_k} , and perform visual feature tracking to obtain series of visual bearing measurements to 3D environmental features. A measurement \mathbf{z}_{c_i} at timestep i is expressed as a function of a cloned pose and feature position ${}^G \mathbf{p}_f$:

$$\mathbf{z}_{c_i} = \mathbf{\Pi}({}^{C_i} \mathbf{p}_f) + \mathbf{n}_i \quad (14)$$

$$\mathbf{\Pi} \left([x \ y \ z]^\top \right) = \begin{bmatrix} \frac{x}{z} & \frac{y}{z} \end{bmatrix}^\top \quad (15)$$

$${}^{C_i} \mathbf{p}_f = {}_I^C \mathbf{R}_{I_G}^{I_i} \mathbf{R} ({}^G \mathbf{p}_f - {}^G \mathbf{p}_{I_i}) + {}^C \mathbf{p}_I \quad (16)$$

where ${}_I^C \mathbf{R}$ and ${}^C \mathbf{p}_I$ represent the camera to IMU extrinsics. To get an estimate of ${}^G \hat{\mathbf{p}}_f$, triangulation is performed using the current state estimates. Then we compute the Jacobian matrix by linearizing Eq. (14) at current estimate and feature position ${}^G \hat{\mathbf{p}}_f = [{}^G \hat{x}_f \quad {}^G \hat{y}_f \quad {}^G \hat{z}_f]^\top$. The Jacobian matrix respect to ${}_{G\bar{q}}^{I_i}$, ${}^G \mathbf{p}_{I_i}$, and ${}^G \mathbf{p}_f$ for the update are:

$$\frac{\partial \tilde{\mathbf{z}}_{c_i}}{\partial {}_{G\bar{q}}^{I_i} \tilde{\boldsymbol{\theta}}} = \mathbf{H}_{pI} {}^C \hat{\mathbf{R}} [{}_{I_G}^{I_i} \hat{\mathbf{R}} ({}^G \hat{\mathbf{p}}_f - {}^G \hat{\mathbf{p}}_{I_i})] \quad \frac{\partial \tilde{\mathbf{z}}_{c_i}}{\partial {}^G \tilde{\mathbf{p}}_{I_i}} = -\mathbf{H}_{pI} {}^C \hat{\mathbf{R}} {}_{I_G}^{I_i} \hat{\mathbf{R}} \quad (17)$$

$$\frac{\partial \tilde{\mathbf{z}}_{c_i}}{\partial^G \tilde{\mathbf{p}}_f} = \mathbf{H}_{pI}^C \hat{\mathbf{R}}_G^{I_i} \hat{\mathbf{R}} \quad \mathbf{H}_p = \begin{bmatrix} \frac{1}{\sigma_i \hat{z}_f} & 0 & -\frac{c_i \hat{x}_f}{\sigma_i \hat{z}_f^2} \\ 0 & \frac{1}{\sigma_i \hat{z}_f} & -\frac{c_i \hat{y}_f}{\sigma_i \hat{z}_f^2} \end{bmatrix} \quad (18)$$

Stacking the Jacobians and residuals for all visual measurements yields the following general form:

$$\tilde{\mathbf{z}}_c = \mathbf{H}_x \tilde{\mathbf{x}}_k + \mathbf{H}_f^G \tilde{\mathbf{p}}_f + \mathbf{n}_f \quad (19)$$

where $\tilde{\mathbf{z}}_c$ is formed by stacking the individual measurement residuals for a given feature, \mathbf{H}_x and \mathbf{H}_f are the state and feature Jacobians, respectively. Either the feature can now be updated using the standard EKF update or treated as a MSCKF feature [5]. The key idea of the MSCKF is to find the matrix $\mathcal{N}(\mathbf{H}_f^\top)$ whose columns span the left null space of \mathbf{H}_f . Multiplying the above linear system on the left by $\mathcal{N}(\mathbf{H}_f^\top)^\top$, we obtain a new measurement function that depends only on the state:

$$\tilde{\mathbf{z}}'_c = \mathbf{H}'_x \tilde{\mathbf{x}}_k + \mathbf{n}'_f \quad (20)$$

We can directly use this measurement in an EKF update without storing features in the state. This leads to substantial computational savings as the problem size remains bounded over the entire trajectory.

2 Wheel-Encoder Measurement Model

Building upon the preceding VIO models, we now generalize our 3D motion tracking system to optimally incorporate 2D wheel-encoder measurements that are commonplace in ground vehicles. In particular, a ground vehicle is often driven by two differential (left and right) wheels mounted on a common axis (baselink), each equipped with an encoder providing local angular rate readings [6]:

$$\omega_{ml} = \omega_l + n_{\omega_l}, \quad \omega_{mr} = \omega_r + n_{\omega_r} \quad (21)$$

where ω_l and ω_r are the true angular velocities of each wheel, and n_{ω_l} and n_{ω_r} are the corresponding zero-mean white Gaussian noises. These encoder readings can be combined to provide 2D linear and angular velocities about the vehicle body or odometer frame $\{O\}$ at the center of the baselink:

$${}^O\omega = (\omega_r r_r - \omega_l r_l)/b, \quad {}^Ov = (\omega_r r_r + \omega_l r_l)/2 \quad (22)$$

where $\mathbf{x}_{WI} := [r_l \ r_r \ b]^\top$ are the left and right wheel radii and the baselink length, respectively.

2.1 Wheel Odometry Preintegration

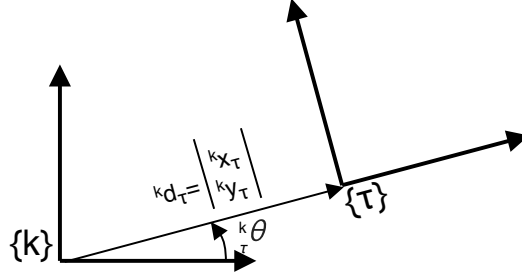


Figure 2: Definition of notations used in 2D

As the wheel encoders typically provide measurements of higher rate (e.g., 100-500 Hz) than the camera, it would be too expensive to perform EKF update at their rate. On the other hand, as a sliding window of states corresponding to the imaging times are stochastically cloned in the state vector [see (1)], we naturally preintegrate the wheel odometry measurements (22) between the two latest camera poses and then use this integrated 2D motion measurement for the MSCKF update together with the visual feature measurements. As a result, the state vector of our VIWO remains the same (up to online calibration) as that of the VIO, incurring only a small extra computational overhead.

Consider preintegrating wheel odometry measurements between two clone times t_k and t_{k+1} . The continuous-time 2D kinematic model for $t_\tau \in [t_k, t_{k+1}]$ is given by:

$$\begin{bmatrix} {}^{O_\tau}\dot{\theta} \\ {}^{O_k}\dot{x}_{O_\tau} \\ {}^{O_k}\dot{y}_{O_\tau} \end{bmatrix} = \begin{bmatrix} -{}^{O_\tau}\omega \\ {}^{O_\tau}v \cos({}^{O_k}\theta) \\ {}^{O_\tau}v \sin({}^{O_k}\theta) \end{bmatrix} = \begin{bmatrix} -{}^{O_\tau}\omega \\ {}^{O_\tau}v \cos({}^{O_\tau}\theta) \\ -{}^{O_\tau}v \sin({}^{O_\tau}\theta) \end{bmatrix} \quad (23)$$

where ${}^{O_k}\theta$ is the local yaw angle, ${}^{O_k}x_{O_\tau}$ and ${}^{O_k}y_{O_\tau}$ are the 2D position of $\{O_\tau\}$ in the starting integration frame $\{O_k\}$. Note that we use $-{}^{O_\tau}\omega$ and $-{}^{O_\tau}v \sin({}^{O_\tau}\theta)$ because we follow global-to-local orientation representation. Also note that this model reveals the fact that the 2D orientation evolves over the integration period.

To locally combine all the wheel odometry measurements from time-step k to $\tau + 1$ without accessing the state estimates (in particular, the orientation), we can perform the following integration of the measurements:

$${}^{O_k}{}_{O_{\tau+1}}\theta = {}^{O_k}{}_{O_{\tau}}\theta - \int_{t_{\tau}}^{t_{\tau+1}} {}^{O_t}\omega dt \quad (24)$$

$$\approx {}^{O_k}{}_{O_{\tau}}\theta - {}^{O_{\tau}}\omega \Delta t \quad (25)$$

$${}^{O_k}x_{O_{\tau+1}} = {}^{O_k}x_{O_{\tau}} + \int_{t_{\tau}}^{t_{\tau+1}} {}^{O_t}v \cos({}^{O_t}\theta) dt \quad (26)$$

$$\approx {}^{O_k}x_{O_{\tau}} + \int_{t_{\tau}}^{t_{\tau+1}} {}^{O_{\tau}}v \cos({}^{O_k}\theta - {}^{O_{\tau}}\omega(t - t_{\tau})) dt \quad (27)$$

$$= {}^{O_k}x_{O_{\tau}} - \frac{{}^{O_{\tau}}v(\sin({}^{O_k}\theta - {}^{O_{\tau}}\omega \Delta t) - \sin({}^{O_k}\theta))}{{}^{O_{\tau}}\omega} \quad (28)$$

$${}^{O_k}y_{O_{\tau+1}} = {}^{O_k}y_{O_{\tau}} - \int_{t_{\tau}}^{t_{\tau+1}} {}^{O_t}v \sin({}^{O_t}\theta) dt \quad (29)$$

$$\approx {}^{O_k}y_{O_{\tau}} - \int_{t_{\tau}}^{t_{\tau+1}} {}^{O_{\tau}}v \sin({}^{O_k}\theta - {}^{O_{\tau}}\omega(t - t_{\tau})) dt \quad (30)$$

$$= {}^{O_k}y_{O_{\tau}} - \frac{{}^{O_{\tau}}v(\cos({}^{O_k}\theta - {}^{O_{\tau}}\omega \Delta t) - \cos({}^{O_k}\theta))}{{}^{O_{\tau}}\omega} \quad (31)$$

where $\Delta t = t_{\tau+1} - t_{\tau}$. Note that we assume constant ${}^{O_{\tau}}\omega$ and ${}^{O_{\tau}}v$ (discrete sensor model) but considered the change of heading angle between t_{τ} and $t_{\tau+1}$ so that we have more accurate model than assuming it constant.

We then integrate these steps from t_k to t_{k+1} and obtain the 2D relative pose measurement as follows:

$$\mathbf{z}_{k+1} = \begin{bmatrix} {}^{O_{k+1}}\theta \\ {}^{O_k}{}_{O_{k+1}}\mathbf{d} \end{bmatrix} = \begin{bmatrix} \int_{t_k}^{t_{k+1}} {}^{O_t}\omega dt \\ \int_{t_k}^{t_{k+1}} {}^{O_t}v \cos({}^{O_t}\theta) dt \\ \int_{t_k}^{t_{k+1}} {}^{O_t}v \sin({}^{O_t}\theta) dt \end{bmatrix} \quad (32)$$

$$=: \mathbf{g}(\omega_{l(k:k+1)}, \omega_{r(k:k+1)}, \mathbf{x}_{WI}) \quad (33)$$

where $\omega_{(k:k+1)}$ denote all the wheel measurements integrated t_k to t_{k+1} . If both extrinsic and time offset (spatiotemporal) calibration parameters between the odometer and IMU/camera are perfectly known, the above integrated odometry measurements can be readily used in the MSCKF update as in [7]. However, in practice, this often is not the case, for example, due to inaccurate prior calibration or mechanical vibration. To cope with possible time-varying calibration parameters during terrain navigation, the proposed VIWO performs online calibration of the wheel-encoders' intrinsics \mathbf{x}_{WI} , and the extrinsics $\mathbf{x}_{WE} = [{}^O\bar{q}^{\top} \quad {}^O\mathbf{p}_I^{\top}]^{\top}$ and time offset ${}^O t_I$ between the odometer and IMU. Note again that the IMU and camera are assumed to be calibrated and synchronized for presentation brevity. To this end, we augment the state vector (1) with these parameters:

$$\mathbf{x}_k = [\mathbf{x}_{I_k}^{\top} \quad \mathbf{x}_{C_k}^{\top} \quad \mathbf{x}_{WE}^{\top} \quad {}^O t_I \quad \mathbf{x}_{WI}^{\top}]^{\top} \quad (34)$$

In what follows, we will derive in detail the relation between the preintegrated wheel odometry measurements (33) and the augmented state (34) by properly taking into account the intrinsic/extrinsic

calibration parameters:

$$\mathbf{z}_{k+1} = \mathbf{h}(\mathbf{x}_{I_{k+1}}, \mathbf{x}_{C_{k+1}}, \mathbf{x}_{WE}, {}^{O_k}t_I, \mathbf{x}_{WI}) \quad (35)$$

2.2 Odometry Measurement wrt. Intrinsic

As evident from (33), the wheel-odometry integration entangles the intrinsic \mathbf{x}_{WI} , and ideally we should re-integrate these measurements whenever a new estimate of intrinsic is available, which however negates the computational efficiency of preintegration. To address this issue, we linearize the preintegrated odometry measurements about the current estimate of the intrinsic while properly taking into account the measurement uncertainty due to the linearization errors of the intrinsic and the noise [see (33)]:

$$\mathbf{z}_{k+1} \simeq \mathbf{g}(\omega_{ml(k:k+1)}, \omega_{mr(k:k+1)}, \hat{\mathbf{x}}_{WI}) + \frac{\partial \mathbf{g}}{\partial \tilde{\mathbf{x}}_{WI}} \tilde{\mathbf{x}}_{WI} + \frac{\partial \mathbf{g}}{\partial \mathbf{n}_w} \mathbf{n}_w \quad (36)$$

where \mathbf{n}_w is the stacked noise vector whose τ -th block is corresponding to the encoder measurement noise at $t_\tau \in [t_k, t_{k+1}]$ (i.e., $[n_{\omega_{l,\tau}} \ n_{\omega_{r,\tau}}]^\top$) [see (21)].

Clearly, performing EKF update with this measurement requires the Jacobians with respect to both the intrinsic and the noise in (36). It is important to note that as the preintegration of $\mathbf{g}(\cdot)$ is computed incrementally using the encoders' measurements in the interval $[t_k, t_{k+1}]$, we accordingly calculate the measurement Jacobians incrementally one step at a time. Note also that since the noise Jacobian and \mathbf{n}_w are often of high dimensions and may be computationally expensive when computing the stacked noise covariance during the update, we instead compute the noise covariance \mathbf{P}_m by performing small matrix operations at each step.

Before we show the derivations of Jacobians and covariance, we would like to show the definition of 2D orientation perturbation that is going to be utilized in derivation. We drive this from general 3D orientation ${}^{O_k} \mathbf{R}$ perturbation as:

$${}^{O_k} \mathbf{R} = \exp(-{}^{O_k} \boldsymbol{\theta}) = \exp({}^{O_k} \tilde{\boldsymbol{\theta}}) \exp(-{}^{O_k} \hat{\boldsymbol{\theta}}) \quad (37)$$

where ${}^{O_k} \boldsymbol{\theta} = {}^{O_k} \theta \mathbf{e}_3$ and \mathbf{e}_i is the i -th standard unit basis vector. Note that we follow JPL notation, that uses $\exp({}^{O_k} \boldsymbol{\theta}) = \exp(-{}^{O_k} \tilde{\boldsymbol{\theta}}) \exp({}^{O_k} \hat{\boldsymbol{\theta}})$. From the above equation we get:

$$\exp({}^{O_k} \tilde{\boldsymbol{\theta}}) = \exp(-{}^{O_k} \boldsymbol{\theta}) \exp(-{}^{O_k} \hat{\boldsymbol{\theta}})^{-1} \quad (38)$$

$$= \begin{bmatrix} \cos({}^{O_k} \theta) & \sin({}^{O_k} \theta) & 0 \\ -\sin({}^{O_k} \theta) & \cos({}^{O_k} \theta) & 0 \\ 0 & 0 & 1 \end{bmatrix} \begin{bmatrix} \cos({}^{O_k} \hat{\theta}) & -\sin({}^{O_k} \hat{\theta}) & 0 \\ \sin({}^{O_k} \hat{\theta}) & \cos({}^{O_k} \hat{\theta}) & 0 \\ 0 & 0 & 1 \end{bmatrix} \quad (39)$$

$$= \begin{bmatrix} \cos({}^{O_k} \theta - {}^{O_k} \hat{\theta}) & \sin({}^{O_k} \theta - {}^{O_k} \hat{\theta}) & 0 \\ -\sin({}^{O_k} \theta - {}^{O_k} \hat{\theta}) & \cos({}^{O_k} \theta - {}^{O_k} \hat{\theta}) & 0 \\ 0 & 0 & 1 \end{bmatrix} \quad (40)$$

$$= \exp({}^{O_k} \hat{\boldsymbol{\theta}} - {}^{O_k} \boldsymbol{\theta}) \quad (41)$$

(41) can be simplified to ${}^{O_k} \tilde{\boldsymbol{\theta}} = {}^{O_k} \hat{\boldsymbol{\theta}} - {}^{O_k} \boldsymbol{\theta}$ by removing the exponential function, and we get the definition of orientation error in 2D as:

$${}^{O_k} \theta = {}^{O_k} \hat{\theta} - {}^{O_k} \tilde{\theta} \quad (42)$$

Using the derivation (42), we get the Jacobian of t_τ step integraion from (25), (28), and (31):

$$\begin{aligned} \frac{O_{\tau+1}}{O_k} \tilde{\theta} &= \frac{O_\tau}{O_k} \tilde{\theta} + \Delta t O_\tau \tilde{\omega} \end{aligned} \quad (43)$$

$$= \frac{O_\tau}{O_k} \tilde{\theta} + h_{\theta\omega} O_\tau \tilde{\omega} \quad (44)$$

$$= \frac{O_\tau}{O_k} \tilde{\theta} + h_{\theta\omega} \mathbf{H}_{\omega\mathbf{x}} \tilde{\mathbf{x}}_{WI} + h_{\theta\omega} \mathbf{H}_{\omega\mathbf{n}} \quad (45)$$

$$= \frac{O_\tau}{O_k} \tilde{\theta} + \mathbf{H}_{1,\tau} \tilde{\mathbf{x}}_{WI} + \mathbf{H}_{2,\tau} \mathbf{n}_{\omega,\tau} \quad (46)$$

$$\begin{aligned} O_k \tilde{x}_{O_{\tau+1}} &= O_k \tilde{x}_{O_\tau} + \frac{O_\tau \hat{v} (\cos(\frac{O_\tau}{O_k} \hat{\theta} - O_\tau \hat{\omega} \Delta t) - \cos(\frac{O_\tau}{O_k} \hat{\theta}))}{O_\tau \hat{\omega}} O_\tau \tilde{\theta} \\ &\quad + \frac{O_\tau \hat{v} (\sin(\frac{O_\tau}{O_k} \hat{\theta} - O_\tau \hat{\omega} \Delta t) - \sin(\frac{O_\tau}{O_k} \hat{\theta}) + O_\tau \hat{\omega} \Delta t \cos(\frac{O_\tau}{O_k} \hat{\theta} - O_\tau \hat{\omega} \Delta t))}{O_\tau \hat{\omega}^2} O_\tau \tilde{\omega} \\ &\quad - \frac{\sin(\frac{O_\tau}{O_k} \hat{\theta} - O_\tau \hat{\omega} \Delta t) - \sin(\frac{O_\tau}{O_k} \hat{\theta})}{O_\tau \hat{\omega}} O_\tau \tilde{v} \end{aligned} \quad (47)$$

$$= O_k \tilde{x}_{O_\tau} + h_{x\theta} \frac{O_\tau}{O_k} \tilde{\theta} + h_{x\omega} O_\tau \tilde{\omega} + h_{xv} O_\tau \tilde{v} \quad (48)$$

$$= O_k \tilde{x}_{O_\tau} + h_{x\theta} \frac{O_\tau}{O_k} \tilde{\theta} + h_{x\omega} (\mathbf{H}_{\omega\mathbf{x}} \tilde{\mathbf{x}}_{WI} + \mathbf{H}_{\omega\mathbf{n}} \mathbf{n}_{\omega,\tau}) + h_{xv} (\mathbf{H}_{v\mathbf{x}} \tilde{\mathbf{x}}_{WI} + \mathbf{H}_{v\mathbf{n}} \mathbf{n}_{\omega,\tau}) \quad (49)$$

$$= O_k \tilde{x}_{O_\tau} + h_{x\theta} \frac{O_\tau}{O_k} \tilde{\theta} + (h_{x\omega} \mathbf{H}_{\omega\mathbf{x}} + h_{xv} \mathbf{H}_{v\mathbf{x}}) \tilde{\mathbf{x}}_{WI} + (h_{x\omega} \mathbf{H}_{\omega\mathbf{n}} + h_{xv} \mathbf{H}_{v\mathbf{n}}) \mathbf{n}_{\omega,\tau} \quad (50)$$

$$= O_k \tilde{x}_{O_\tau} + \mathbf{H}_{3,\tau} \frac{O_\tau}{O_k} \tilde{\theta} + \mathbf{H}_{4,\tau} \tilde{\mathbf{x}}_{WI} + \mathbf{H}_{5,\tau} \quad (51)$$

$$\begin{aligned} O_k \tilde{y}_{O_{\tau+1}} &= O_k \tilde{y}_{O_\tau} - \frac{O_\tau \hat{v} (\sin(\frac{O_\tau}{O_k} \hat{\theta} - O_\tau \hat{\omega} \Delta t) - \sin(\frac{O_\tau}{O_k} \hat{\theta}))}{O_\tau \hat{\omega}} O_\tau \tilde{\theta} \\ &\quad + \frac{O_\tau \hat{v} (\cos(\frac{O_\tau}{O_k} \hat{\theta} - O_\tau \hat{\omega} \Delta t) - \cos(\frac{O_\tau}{O_k} \hat{\theta}) - O_\tau \hat{\omega} \Delta t \sin(\frac{O_\tau}{O_k} \hat{\theta} - O_\tau \hat{\omega} \Delta t))}{O_\tau \hat{\omega}^2} O_\tau \tilde{\omega} \\ &\quad - \frac{\cos(\frac{O_\tau}{O_k} \hat{\theta} - O_\tau \hat{\omega} \Delta t) - \cos(\frac{O_\tau}{O_k} \hat{\theta})}{O_\tau \hat{\omega}} O_\tau \tilde{v} \end{aligned} \quad (52)$$

$$= O_k \tilde{y}_{O_\tau} + h_{y\theta} \frac{O_\tau}{O_k} \tilde{\theta} + h_{y\omega} O_\tau \tilde{\omega} + h_{yv} O_\tau \tilde{v} \quad (53)$$

$$= O_k \tilde{y}_{O_\tau} + h_{y\theta} \frac{O_\tau}{O_k} \tilde{\theta} + h_{y\omega} (\mathbf{H}_{\omega\mathbf{x}} \tilde{\mathbf{x}}_{WI} + \mathbf{H}_{\omega\mathbf{n}} \mathbf{n}_{\omega,\tau}) + h_{yv} (\mathbf{H}_{v\mathbf{x}} \tilde{\mathbf{x}}_{WI} + \mathbf{H}_{v\mathbf{n}} \mathbf{n}_{\omega,\tau}) \quad (54)$$

$$= O_k \tilde{y}_{O_\tau} + h_{y\theta} \frac{O_\tau}{O_k} \tilde{\theta} + (h_{y\omega} \mathbf{H}_{\omega\mathbf{x}} + h_{yv} \mathbf{H}_{v\mathbf{x}}) \tilde{\mathbf{x}}_{WI} + (h_{y\omega} \mathbf{H}_{\omega\mathbf{n}} + h_{yv} \mathbf{H}_{v\mathbf{n}}) \mathbf{n}_{\omega,\tau} \quad (55)$$

$$= O_k \tilde{y}_{O_\tau} + \mathbf{H}_{6,\tau} \frac{O_\tau}{O_k} \tilde{\theta} + \mathbf{H}_{7,\tau} \tilde{\mathbf{x}}_{WI} + \mathbf{H}_{8,\tau} \mathbf{n}_{\omega,\tau} \quad (56)$$

where $\mathbf{H}_{\omega\mathbf{x}}$, $\mathbf{H}_{\omega\mathbf{n}}$, $\mathbf{H}_{v\mathbf{x}}$, and $\mathbf{H}_{v\mathbf{n}}$ are the Jacobians of measurement (22) respect to intrinsic and the noise with given estimate values as:

$$O \tilde{\omega} = \begin{bmatrix} \frac{-\omega_{ml}}{\hat{b}} & \frac{\omega_{mr}}{\hat{b}} & -\frac{\omega_{mr} \hat{r}_r - \omega_{ml} \hat{r}_l}{\hat{b}^2} \end{bmatrix} \begin{bmatrix} \tilde{r}_l \\ \tilde{r}_r \\ \tilde{b} \end{bmatrix} + \begin{bmatrix} \hat{r}_l & -\hat{r}_r \end{bmatrix} \begin{bmatrix} n_{\omega_l} \\ n_{\omega_r} \end{bmatrix} \quad (57)$$

$$= \mathbf{H}_{\omega\mathbf{x}} \tilde{\mathbf{x}}_{CI} + \mathbf{H}_{\omega\mathbf{n}} \mathbf{n}_\omega \quad (58)$$

$$O \tilde{v} = \begin{bmatrix} \frac{\omega_{ml}}{2} & \frac{\omega_{mr}}{2} & 0 \end{bmatrix} \begin{bmatrix} \tilde{r}_l \\ \tilde{r}_r \\ \tilde{b} \end{bmatrix} + \begin{bmatrix} -\hat{r}_l & -\hat{r}_r \end{bmatrix} \begin{bmatrix} n_{\omega_l} \\ n_{\omega_r} \end{bmatrix} \quad (59)$$

$$= \mathbf{H}_{v\mathbf{x}} \tilde{\mathbf{x}}_{CI} + \mathbf{H}_{v\mathbf{n}} \mathbf{n}_\omega \quad (60)$$

It can be found that the error of $\tau + 1$ step preintegration is the linear combination of τ step preintegration and measurement errors. With the above equations, we can recursively compute the noise covariance $\mathbf{P}_{m,\tau+1}$ and the Jacobian $\frac{\partial \mathbf{g}_{\tau+1}}{\partial \tilde{\mathbf{x}}_{WI}}$ as follows:

$$\Phi_{tr,\tau} = \begin{bmatrix} 1 & 0 & 0 \\ \mathbf{H}_{3,\tau} & 1 & 0 \\ \mathbf{H}_{6,\tau} & 0 & 1 \end{bmatrix}, \quad \Phi_{WI,\tau} = \begin{bmatrix} \mathbf{H}_{1,\tau} \\ \mathbf{H}_{4,\tau} \\ \mathbf{H}_{7,\tau} \end{bmatrix}, \quad \Phi_{n,\tau} = \begin{bmatrix} \mathbf{H}_{2,\tau} \\ \mathbf{H}_{5,\tau} \\ \mathbf{H}_{8,\tau} \end{bmatrix} \quad (61)$$

$$\mathbf{P}_{m,\tau+1} = \Phi_{tr,\tau} \mathbf{P}_{m,\tau} \Phi_{tr,\tau}^\top + \Phi_{n,\tau} \mathbf{Q}_\tau \Phi_{n,\tau}^\top \quad (62)$$

$$\frac{\partial \mathbf{g}_{\tau+1}}{\partial \tilde{\mathbf{x}}_{WI}} = \Phi_{tr,\tau} \frac{\partial \mathbf{g}_\tau}{\partial \tilde{\mathbf{x}}_{WI}} + \Phi_{WI,\tau} \quad (63)$$

where \mathbf{Q}_τ is the noise covariance of wheel encoder measurement at t_τ . These equations show how the Jacobian and the noise covariance evolve during the preintegration interval. We thus can recursively compute measurement noise covariance \mathbf{P}_m and the Jacobian matrix $\frac{\partial \mathbf{g}}{\partial \tilde{\mathbf{x}}_{WI}}$ at the end of preintegration t_{k+1} , based on the zero initial condition (i.e., $\mathbf{P}_{m,0}, \frac{\partial \mathbf{g}_0}{\partial \tilde{\mathbf{x}}_{WI}} = \mathbf{0}_3$). The closed form of $\frac{\partial \mathbf{g}}{\partial \tilde{\mathbf{x}}_{WI}}$ can be derived by assuming n number of measurements are used for preintegration as:

$$O_k^{k+1} \tilde{\theta} = \sum_{i=1}^n h_{\theta\omega,i} \mathbf{H}_{\omega\mathbf{x},i} \tilde{\mathbf{x}}_{CI} \quad (64)$$

$$= \sum_{i=1}^n \Delta t_i \begin{bmatrix} -\frac{\omega_{ml,i}}{\hat{b}} & \frac{\omega_{mr,i}}{\hat{b}} & -\frac{\omega_{mr,i} \hat{r}_r - \omega_{ml,i} \hat{r}_l}{\hat{b}^2} \end{bmatrix} \tilde{\mathbf{x}}_{CI} \quad (65)$$

$$= [\mathbf{\Gamma}_{\theta 1} \quad \mathbf{\Gamma}_{\theta 2} \quad \mathbf{\Gamma}_{\theta 3}] \tilde{\mathbf{x}}_{CI} \quad (66)$$

$$O_k \tilde{x}_{O_{k+1}} = \sum_{i=1}^n h_{x\theta,i} O_k^i \tilde{\theta} + (h_{x\omega,i} \mathbf{H}_{\omega\mathbf{x},i} + h_{xv,i} \mathbf{H}_{v\mathbf{x},i}) \tilde{\mathbf{x}}_{CI} \quad (67)$$

$$= \sum_{i=1}^n h_{x\theta,i} \left\{ \sum_{j=1}^{i-1} \Delta t_j \begin{bmatrix} -\frac{\omega_{ml,j}}{\hat{b}} & \frac{\omega_{mr,j}}{\hat{b}} & -\frac{\omega_{mr,j} \hat{r}_r - \omega_{ml,j} \hat{r}_l}{\hat{b}^2} \end{bmatrix} \tilde{\mathbf{x}}_{CI} \right\} \\ + (h_{x\omega,i} \begin{bmatrix} -\frac{\omega_{ml,i}}{\hat{b}} & \frac{\omega_{mr,i}}{\hat{b}} & -\frac{\omega_{mr,i} \hat{r}_r - \omega_{ml,i} \hat{r}_l}{\hat{b}^2} \end{bmatrix} + h_{xv,i} \begin{bmatrix} \frac{\omega_{ml,i}}{2} & \frac{\omega_{mr,i}}{2} & 0 \end{bmatrix}) \tilde{\mathbf{x}}_{CI} \quad (68)$$

$$= [\mathbf{\Gamma}_{x1} \quad \mathbf{\Gamma}_{x2} \quad \mathbf{\Gamma}_{x3}] \tilde{\mathbf{x}}_{CI} \quad (69)$$

$$O_k \tilde{y}_{O_{k+1}} = \sum_{i=1}^n h_{y\theta,i} O_k^i \tilde{\theta} + (h_{y\omega,i} \mathbf{H}_{\omega\mathbf{x},i} + h_{yv,i} \mathbf{H}_{v\mathbf{x},i}) \tilde{\mathbf{x}}_{CI} \quad (70)$$

$$= \sum_{i=1}^n h_{y\theta,i} \left\{ \sum_{j=1}^{i-1} \Delta t_j \begin{bmatrix} -\frac{\omega_{ml,j}}{\hat{b}} & \frac{\omega_{mr,j}}{\hat{b}} & -\frac{\omega_{mr,j} \hat{r}_r - \omega_{ml,j} \hat{r}_l}{\hat{b}^2} \end{bmatrix} \tilde{\mathbf{x}}_{CI} \right\} \\ + (h_{y\omega,i} \begin{bmatrix} -\frac{\omega_{ml,i}}{\hat{b}} & \frac{\omega_{mr,i}}{\hat{b}} & -\frac{\omega_{mr,i} \hat{r}_r - \omega_{ml,i} \hat{r}_l}{\hat{b}^2} \end{bmatrix} + h_{yv,i} \begin{bmatrix} \frac{\omega_{ml,i}}{2} & \frac{\omega_{mr,i}}{2} & 0 \end{bmatrix}) \tilde{\mathbf{x}}_{CI} \quad (71)$$

$$= [\mathbf{\Gamma}_{y1} \quad \mathbf{\Gamma}_{y2} \quad \mathbf{\Gamma}_{y3}] \tilde{\mathbf{x}}_{CI} \quad (72)$$

where

$$\mathbf{\Gamma}_{\theta 1} = \sum_{i=1}^n -\Delta t_i \frac{\omega_{ml,i}}{\hat{b}} \quad (73)$$

$$\Gamma_{\theta 2} = \sum_{i=1}^n \Delta t_i \frac{\omega_{mr,i}}{\hat{b}} \quad (74)$$

$$\Gamma_{\theta 3} = \sum_{i=1}^n -\Delta t_i \frac{\omega_{mr,i} \hat{r}_r - \omega_{ml,i} \hat{r}_l}{\hat{b}^2} \quad (75)$$

$$\Gamma_{\mathbf{x}1} = \sum_{i=1}^n \left\{ -h_{x\omega,i} \frac{\omega_{ml,i}}{\hat{b}} + h_{xv,i} \frac{\omega_{ml,i}}{2} - h_{x\theta,i} \sum_{j=1}^{i-1} \Delta t_j \frac{\omega_{ml,j}}{\hat{b}} \right\} \quad (76)$$

$$\Gamma_{\mathbf{x}2} = \sum_{i=1}^n \left\{ h_{x\omega,i} \frac{\omega_{mr,i}}{\hat{b}} + h_{xv,i} \frac{\omega_{mr,i}}{2} + h_{x\theta,i} \sum_{j=1}^{i-1} \Delta t_j \frac{\omega_{mr,j}}{\hat{b}} \right\} \quad (77)$$

$$\Gamma_{\mathbf{x}3} = \sum_{i=1}^n \left\{ -h_{x\omega,i} \frac{\omega_{mr,i} \hat{r}_r - \omega_{ml,i} \hat{r}_l}{\hat{b}^2} - h_{x\theta,i} \sum_{j=1}^{i-1} \Delta t_j \frac{\omega_{mr,j} \hat{r}_r - \omega_{ml,j} \hat{r}_l}{\hat{b}^2} \right\} \quad (78)$$

$$\Gamma_{\mathbf{y}1} = \sum_{i=1}^n \left\{ -h_{y\omega,i} \frac{\omega_{ml,i}}{\hat{b}} + h_{yv,i} \frac{\omega_{ml,i}}{2} - h_{y\theta,i} \sum_{j=1}^{i-1} \Delta t_j \frac{\omega_{ml,j}}{\hat{b}} \right\} \quad (79)$$

$$\Gamma_{\mathbf{y}2} = \sum_{i=1}^n \left\{ h_{y\omega,i} \frac{\omega_{mr,i}}{\hat{b}} + h_{yv,i} \frac{\omega_{mr,i}}{2} + h_{y\theta,i} \sum_{j=1}^{i-1} \Delta t_j \frac{\omega_{mr,j}}{\hat{b}} \right\} \quad (80)$$

$$\Gamma_{\mathbf{y}3} = \sum_{i=1}^n \left\{ -h_{y\omega,i} \frac{\omega_{mr,i} \hat{r}_r - \omega_{ml,i} \hat{r}_l}{\hat{b}^2} - h_{y\theta,i} \sum_{j=1}^{i-1} \Delta t_j \frac{\omega_{mr,j} \hat{r}_r - \omega_{ml,j} \hat{r}_l}{\hat{b}^2} \right\} \quad (81)$$

To summarize, we get the Jacobian of intrinsic state as:

$$\frac{\partial \mathbf{g}}{\partial \tilde{\mathbf{x}}_{WI}} = \begin{bmatrix} \Gamma_{\theta 1} & \Gamma_{\theta 2} & \Gamma_{\theta 3} \\ \Gamma_{\mathbf{x}1} & \Gamma_{\mathbf{x}2} & \Gamma_{\mathbf{x}3} \\ \Gamma_{\mathbf{y}1} & \Gamma_{\mathbf{y}2} & \Gamma_{\mathbf{y}3} \end{bmatrix} \quad (82)$$

Note this derivation cannot be applied in computing covariance matrix \mathbf{P}_m , because the noise $\mathbf{n}_{\omega,\tau}$ has different values for every iteration unlike $\tilde{\mathbf{x}}_{WI}$.

2.3 Odometry Measurement wrt. Extrinsic

2.3.1 Spatial calibration

Note that the preintegrated wheel measurement (33) provides *only* the 2D relative motion on the odometer's plane, while the VIWO state vector (34) contains the 3D IMU/camera poses. In order to establish the connection of the preintegrated odometry with the state, clearly the relative transformation (extrinsic calibration) between the IMU and the odometer is required [see (32)]:

$$\mathbf{z}_{k+1} = \begin{bmatrix} O_{k+1} \theta \\ O_k \\ O_k \mathbf{d}_{O_{k+1}} \end{bmatrix} = \begin{bmatrix} \mathbf{e}_3^\top \text{Log}(O_I^O \mathbf{R}_G^{I_{k+1}} \mathbf{R}_G^{I_k} \mathbf{R}_I^\top O \mathbf{R}^\top) \\ \Lambda_I^O \mathbf{R}_G^{I_k} \mathbf{R} ({}^G \mathbf{p}_{I_{k+1}} + {}^{I_{k+1}} \mathbf{R}^\top I \mathbf{p}_O - {}^G \mathbf{p}_{I_k} - {}^I_k \mathbf{R}^\top I \mathbf{p}_O) \end{bmatrix} \quad (83)$$

where $\Lambda = [\mathbf{e}_1 \ \mathbf{e}_2]^\top$ and $\text{Log}(\cdot)$ is the $SO(3)$ matrix logarithm function [8]. As this measurement depends on the two consecutive poses as well as the odometer/IMU extrinsics, when updating with it in the MSCKF, the measurement residual and the corresponding measurement Jacobians are needed and computed as follows.

The residual of each measurement can be defined as:

$$\mathbf{r}_\theta = \mathbf{e}_3^\top \text{Log}({}_I^O \hat{\mathbf{R}}_G^{I_{k+1}} \hat{\mathbf{R}}_G^{I_k} \hat{\mathbf{R}}_I^{O \hat{\mathbf{R}}^\top}) - \frac{O_{k+1}}{O_k} \quad (84)$$

$$\mathbf{r}_d = {}^{O_k} \mathbf{d}_{O_{k+1}} - \Lambda_I^O \hat{\mathbf{R}}_G^{I_k} \hat{\mathbf{R}}_G^{I_{k+1}} ({}^G \hat{\mathbf{p}}_{I_{k+1}} + {}_G^{I_{k+1}} \hat{\mathbf{R}}^\top I \hat{\mathbf{p}}_O - {}^G \hat{\mathbf{p}}_{I_k} - {}_G^{I_k} \hat{\mathbf{R}}^\top I \hat{\mathbf{p}}_O) \quad (85)$$

Note that we have *prediction - measurement* form in orientation residual because of the definition of 2D orientation perturbation (42).

First, we perturb the poses to get the Jacobian matrix of (83) respect to the poses as:

$$(\mathbf{I} - [\mathbf{e}_3^{\top O_{k+1}} \tilde{\theta}])_{O_k}^{O_{k+1}} \hat{\mathbf{R}} = {}_I^O \hat{\mathbf{R}} (\mathbf{I} - [{}_G^{I_{k+1}} \tilde{\theta}])_G^{I_{k+1}} \hat{\mathbf{R}}_G^{I_k} \hat{\mathbf{R}}^\top (\mathbf{I} + [{}_G^{I_k} \tilde{\theta}])_I^O \hat{\mathbf{R}}^\top \quad (86)$$

$${}_{O_k}^{O_{k+1}} \tilde{\theta} \approx \mathbf{e}_3^\top {}_I^O \hat{\mathbf{R}}_G^{I_{k+1}} \tilde{\theta} - \mathbf{e}_3^\top {}_I^O \hat{\mathbf{R}}_G^{I_{k+1}} \hat{\mathbf{R}}_G^{I_k} \hat{\mathbf{R}}^\top I {}_G^{I_k} \tilde{\theta} \quad (87)$$

$$\begin{aligned} {}^{O_k} \hat{\mathbf{d}}_{O_{k+1}} + {}^{O_k} \tilde{\mathbf{d}}_{O_{k+1}} &= \Lambda_I^O \hat{\mathbf{R}} (\mathbf{I} - [{}_G^{I_k} \tilde{\theta}])_G^{I_k} \hat{\mathbf{R}} ({}^G \hat{\mathbf{p}}_{I_{k+1}} + {}^G \tilde{\mathbf{p}}_{I_{k+1}}) \\ &\quad + \Lambda_I^O \hat{\mathbf{R}} (\mathbf{I} - [{}_G^{I_k} \tilde{\theta}])_G^{I_k} \hat{\mathbf{R}}_G^{I_{k+1}} \hat{\mathbf{R}}^\top (\mathbf{I} + [{}_G^{I_{k+1}} \tilde{\theta}])_I^O \hat{\mathbf{p}}_O \\ &\quad - \Lambda_I^O \hat{\mathbf{R}} (\mathbf{I} - [{}_G^{I_k} \tilde{\theta}])_G^{I_k} \hat{\mathbf{R}} ({}^G \hat{\mathbf{p}}_{I_k} + {}^G \tilde{\mathbf{p}}_{I_k}) - {}_I^O \hat{\mathbf{R}} I \hat{\mathbf{p}}_O \end{aligned} \quad (88)$$

$$\begin{aligned} {}^{O_k} \tilde{\mathbf{d}}_{O_{k+1}} &\approx \Lambda_I^O \hat{\mathbf{R}} [{}_G^{I_k} \hat{\mathbf{R}} ({}^G \hat{\mathbf{p}}_{I_{k+1}} + {}_G^{I_{k+1}} \hat{\mathbf{R}}^\top I \hat{\mathbf{p}}_O - {}^G \hat{\mathbf{p}}_{I_k})]_G^{I_k} \tilde{\theta} \\ &\quad - \Lambda_I^O \hat{\mathbf{R}}_G^{I_k} \hat{\mathbf{R}}^G \tilde{\mathbf{p}}_{I_k} - \Lambda_I^O \hat{\mathbf{R}}_G^{I_k} \hat{\mathbf{R}}_G^{I_{k+1}} \hat{\mathbf{R}}^\top [I \hat{\mathbf{p}}_O]_G^{I_{k+1}} \tilde{\theta} + \Lambda_I^O \hat{\mathbf{R}}_G^{I_k} \hat{\mathbf{R}}^G \tilde{\mathbf{p}}_{I_{k+1}} \end{aligned} \quad (89)$$

Also, the perturbation of the spatial extrinsic is:

$$(\mathbf{I} - [\mathbf{e}_3^{\top O_{k+1}} \tilde{\theta}])_{O_k}^{O_{k+1}} \hat{\mathbf{R}} = (\mathbf{I} - [{}_I^O \tilde{\theta}])_I^O \hat{\mathbf{R}}_G^{I_{k+1}} \hat{\mathbf{R}}_G^{I_k} \hat{\mathbf{R}}^\top I \hat{\mathbf{R}}^\top (\mathbf{I} + [{}_I^O \tilde{\theta}]) \quad (90)$$

$${}_{O_k}^{O_{k+1}} \tilde{\theta} \approx \mathbf{e}_3^\top (\mathbf{I} - {}_I^O \hat{\mathbf{R}}_G^{I_{k+1}} \hat{\mathbf{R}}_G^{I_k} \hat{\mathbf{R}}^\top I \hat{\mathbf{R}}^\top) {}_I^O \tilde{\theta} \quad (91)$$

$$\begin{aligned} {}^{O_k} \hat{\mathbf{d}}_{O_{k+1}} + {}^{O_k} \tilde{\mathbf{d}}_{O_{k+1}} &= \Lambda (\mathbf{I} - [{}_I^O \tilde{\theta}])_I^O \hat{\mathbf{R}}_G^{I_k} \hat{\mathbf{R}}^G \hat{\mathbf{p}}_{I_{k+1}} \\ &\quad - \Lambda (\mathbf{I} - [{}_I^O \tilde{\theta}])_I^O \hat{\mathbf{R}}_G^{I_k} \hat{\mathbf{R}}_G^{I_{k+1}} \hat{\mathbf{R}}^\top I \hat{\mathbf{R}}^\top (\mathbf{I} + [{}_I^O \tilde{\theta}]) ({}^O \hat{\mathbf{p}}_I + {}^O \tilde{\mathbf{p}}_I) \\ &\quad - \Lambda (\mathbf{I} - [{}_I^O \tilde{\theta}])_I^O \hat{\mathbf{R}}_G^{I_k} \hat{\mathbf{R}}^G \hat{\mathbf{p}}_{I_k} + \Lambda ({}^O \hat{\mathbf{p}}_I + {}^O \tilde{\mathbf{p}}_I) \end{aligned} \quad (92)$$

$$\begin{aligned} {}^{O_k} \tilde{\mathbf{d}}_{O_{k+1}} &\approx \Lambda ([{}_I^O \hat{\mathbf{R}}_G^{I_k} \hat{\mathbf{R}} ({}^G \hat{\mathbf{p}}_{I_{k+1}} + {}_G^{I_{k+1}} \hat{\mathbf{R}}^\top I \hat{\mathbf{p}}_O - {}^G \hat{\mathbf{p}}_{I_k})] + {}_I^O \hat{\mathbf{R}}_G^{I_k} \hat{\mathbf{R}}_G^{I_{k+1}} \hat{\mathbf{R}}^\top I \hat{\mathbf{R}}^\top [{}^O \hat{\mathbf{p}}_I])_I^O \tilde{\theta} \\ &\quad + \Lambda (\mathbf{I} - {}_I^O \hat{\mathbf{R}}_G^{I_k} \hat{\mathbf{R}}_G^{I_{k+1}} \hat{\mathbf{R}}^\top I \hat{\mathbf{R}}^\top) {}_I^O \tilde{\mathbf{p}}_I \end{aligned} \quad (93)$$

By collecting the above equations into the matrix shape, we get the following Jacobian matrix respect to the each state as:

$$\frac{\partial \mathbf{h}}{\partial \tilde{\mathbf{x}}_{I_{k+1}}} = \begin{bmatrix} \mathbf{e}_3^\top {}_I^O \hat{\mathbf{R}} & \mathbf{0}_{1 \times 3} & \mathbf{0}_{1 \times 9} \\ -\Lambda_I^O \hat{\mathbf{R}}_G^{I_k} \hat{\mathbf{R}}_G^{I_{k+1}} \hat{\mathbf{R}}^\top [I \hat{\mathbf{p}}_O] & \Lambda_I^O \hat{\mathbf{R}}_G^{I_k} \hat{\mathbf{R}} & \mathbf{0}_{2 \times 9} \end{bmatrix} \quad (94)$$

$$\frac{\partial \mathbf{h}}{\partial \tilde{\mathbf{x}}_{C_{k+1}}} = \begin{bmatrix} -\mathbf{e}_3^\top {}_I^O \hat{\mathbf{R}}_G^{I_{k+1}} \hat{\mathbf{R}}_G^{I_k} \hat{\mathbf{R}}^\top & \mathbf{0}_{1 \times 3} \\ \Lambda_I^O \hat{\mathbf{R}} [{}_G^{I_k} \hat{\mathbf{R}} ({}^G \hat{\mathbf{p}}_{I_{k+1}} + {}_G^{I_{k+1}} \hat{\mathbf{R}}^\top I \hat{\mathbf{p}}_O - {}^G \hat{\mathbf{p}}_{I_k})] & -\Lambda_I^O \hat{\mathbf{R}}_G^{I_k} \hat{\mathbf{R}} \end{bmatrix} \quad (95)$$

$$\frac{\partial \mathbf{h}}{\partial \tilde{\mathbf{x}}_{WE}} = \begin{bmatrix} \mathbf{e}_3^\top (\mathbf{I} - {}_I^O \hat{\mathbf{R}}_G^{I_{k+1}} \hat{\mathbf{R}}_G^{I_k} \hat{\mathbf{R}}^\top I \hat{\mathbf{R}}^\top) & \mathbf{0}_{1 \times 3} \\ \mathbf{H}_{WE1} & \Lambda (\mathbf{I} - {}_I^O \hat{\mathbf{R}}_G^{I_k} \hat{\mathbf{R}}_G^{I_{k+1}} \hat{\mathbf{R}}^\top I \hat{\mathbf{R}}^\top) \end{bmatrix} \quad (96)$$

$$\mathbf{H}_{WE1} = \Lambda ([{}_I^O \hat{\mathbf{R}}_G^{I_k} \hat{\mathbf{R}} ({}^G \hat{\mathbf{p}}_{I_{k+1}} + {}_G^{I_{k+1}} \hat{\mathbf{R}}^\top I \hat{\mathbf{p}}_O - {}^G \hat{\mathbf{p}}_{I_k})] + {}_I^O \hat{\mathbf{R}}_G^{I_k} \hat{\mathbf{R}}_G^{I_{k+1}} \hat{\mathbf{R}}^\top I \hat{\mathbf{R}}^\top [{}^O \hat{\mathbf{p}}_I]) \quad (97)$$

Note that the Jacobians (94) and (95) are the same with [7].

2.3.2 Temporal calibration

To account for the difference between sensor clocks and measurement delay, we model an unknown constant time offset between the IMU clock and the odometer clock:¹ ${}^I t_k = {}^O t_k + {}^O t_I$, where ${}^I t_k$ and ${}^O t_k$ are the times when measurement \mathbf{z}_k was collected in the IMU and odometer's clocks, and ${}^O t_I$ is the time offset between the two time references. Consider that we want to derive preintegrated odometry constraints between two cloned states at the true IMU times ${}^I t_k$ and ${}^I t_{k+1}$. Using the current best estimate of the time offset ${}^O \hat{t}_I$, we can integrate our wheel encoder measurements between the odometer times ${}^O t_k = {}^I t_k - {}^O \hat{t}_I$ and ${}^O t_{k+1} = {}^I t_{k+1} - {}^O \hat{t}_I$, whose corresponding times in the IMU clock are:

$${}^I t'_k := {}^I t_k - {}^O \hat{t}_I + {}^O t_I = {}^I t_k + {}^O \tilde{t}_I \quad (98)$$

$${}^I t'_{k+1} := {}^I t_{k+1} - {}^O \hat{t}_I + {}^O t_I = {}^I t_{k+1} + {}^O \tilde{t}_I \quad (99)$$

After preintegration we have the 2D relative pose measurement between the times ${}^I t'_k$ and ${}^I t'_{k+1}$ while the corresponding states are at the times ${}^I t_k$ and ${}^I t_{k+1}$. To update with this measurement, we employ the following first-order approximation by accounting the time-offset estimation error:

$${}^G \mathbf{R}^{(I t'_k)} = {}^G \mathbf{R}^{(I t_k + {}^O \tilde{t}_I)} \quad (100)$$

$$\approx (\mathbf{I} - [{}^{I(I t_k)} \boldsymbol{\omega} {}^O \tilde{t}_I])_G^{I(I t_k)} \mathbf{R} \quad (101)$$

$$= (\mathbf{I} - [{}^{I k} \boldsymbol{\omega} {}^O \tilde{t}_I])_G^{I k} \mathbf{R} \quad (102)$$

$${}^G \mathbf{p}_{I(I t'_k)} = {}^G \mathbf{p}_{I(I t_k + {}^O \tilde{t}_I)} \quad (103)$$

$$\approx {}^G \mathbf{p}_{I(I t_k)} + {}^G \mathbf{v}_{I(I t_k)} {}^O \tilde{t}_I \quad (104)$$

$$= {}^G \mathbf{p}_{I k} + {}^G \mathbf{v}_{I k} {}^O \tilde{t}_I \quad (105)$$

Then the perturbation of the measurement become:

$$(\mathbf{I} - [\mathbf{e}_3^{O_{k+1}} \tilde{\theta}])_{O_k}^{O_{k+1}} \hat{\mathbf{R}} \approx {}^O \hat{\mathbf{R}} (\mathbf{I} - [{}^{I_{k+1}} \boldsymbol{\omega} {}^O \tilde{t}_I])_G^{I_{k+1}} \hat{\mathbf{R}}_G^{I k} \hat{\mathbf{R}}^\top (\mathbf{I} + [{}^{I k} \boldsymbol{\omega} {}^O \tilde{t}_I])_I^O \hat{\mathbf{R}}^\top \quad (106)$$

$$\approx {}^O \hat{\mathbf{R}}_G^{I_{k+1}} \hat{\mathbf{R}}_G^{I k} \hat{\mathbf{R}}^\top {}^O \hat{\mathbf{R}}^\top - {}^O \hat{\mathbf{R}} [{}^{I_{k+1}} \boldsymbol{\omega} {}^O \tilde{t}_I]_G^{I_{k+1}} \hat{\mathbf{R}}_G^{I k} \hat{\mathbf{R}}^\top {}^O \hat{\mathbf{R}}^\top + {}^O \hat{\mathbf{R}}_G^{I_{k+1}} \hat{\mathbf{R}}_G^{I k} \hat{\mathbf{R}}^\top [{}^{I k} \boldsymbol{\omega} {}^O \tilde{t}_I]_I^O \hat{\mathbf{R}}^\top \quad (107)$$

$${}^O_{O_k} \tilde{\theta} \approx \mathbf{e}_3^\top {}^O \hat{\mathbf{R}} ({}^{I_{k+1}} \boldsymbol{\omega} - {}^G \hat{\mathbf{R}}_G^{I k} \hat{\mathbf{R}}^\top {}^{I k} \boldsymbol{\omega}) {}^O \tilde{t}_I \quad (108)$$

$$\begin{aligned} {}^O_k \hat{\mathbf{d}}_{O_{k+1}} + {}^O_k \tilde{\mathbf{d}}_{O_{k+1}} &= \Lambda_I^O \hat{\mathbf{R}} (\mathbf{I} - [{}^{I k} \boldsymbol{\omega} {}^O \tilde{t}_I])_G^{I k} \hat{\mathbf{R}} ({}^G \hat{\mathbf{p}}_{I_{k+1}} + {}^G \hat{\mathbf{v}}_{I_{k+1}} {}^O \tilde{t}_I) \\ &\quad + \Lambda_I^O \hat{\mathbf{R}} (\mathbf{I} - [{}^{I k} \boldsymbol{\omega} {}^O \tilde{t}_I])_G^{I k} \hat{\mathbf{R}}_G^{I_{k+1}} \hat{\mathbf{R}}^\top (\mathbf{I} + [{}^{I_{k+1}} \boldsymbol{\omega} {}^O \tilde{t}_I])_I^O \hat{\mathbf{p}}_O \\ &\quad - \Lambda_I^O \hat{\mathbf{R}} (\mathbf{I} - [{}^{I k} \boldsymbol{\omega} {}^O \tilde{t}_I])_G^{I k} \hat{\mathbf{R}} ({}^G \hat{\mathbf{p}}_{I k} + {}^G \hat{\mathbf{v}}_{I k} {}^O \tilde{t}_I) - \Lambda_I^O \hat{\mathbf{R}}^I \hat{\mathbf{p}}_O \end{aligned} \quad (109)$$

$$\begin{aligned} {}^O_k \tilde{\mathbf{d}}_{O_{k+1}} &\approx \Lambda_I^O \hat{\mathbf{R}} [{}^G \hat{\mathbf{R}}_G^{I k} \hat{\mathbf{p}}_{I_{k+1}} + {}^G \hat{\mathbf{R}}_G^{I_{k+1}} \hat{\mathbf{R}}^\top {}^I \hat{\mathbf{p}}_O - {}^G \hat{\mathbf{R}}_G^{I k} \hat{\mathbf{p}}_{I k}] {}^{I k} \boldsymbol{\omega} \\ &\quad + {}^O \hat{\mathbf{R}}_G^{I k} \hat{\mathbf{R}}_G^{I k} \hat{\mathbf{R}}^\top \hat{\mathbf{v}}_{I_{k+1}} - {}^O \hat{\mathbf{R}}_G^{I k} \hat{\mathbf{R}}_G^{I_{k+1}} \hat{\mathbf{R}}^\top [{}^I \hat{\mathbf{p}}_O]^{I_{k+1}} \boldsymbol{\omega} - {}^O \hat{\mathbf{R}}_G^{I k} \hat{\mathbf{R}}_G^{I k} \hat{\mathbf{R}}^\top \hat{\mathbf{v}}_{I k} {}^O \tilde{t}_I \end{aligned} \quad (110)$$

Therefore the Jacobian of temporal extrinsic become:

$$\frac{\partial \mathbf{h}}{\partial {}^O \tilde{t}_I} = \begin{bmatrix} \mathbf{e}_3^\top {}^O \hat{\mathbf{R}} ({}^{I_{k+1}} \boldsymbol{\omega} - {}^G \hat{\mathbf{R}}_G^{I k} \hat{\mathbf{R}}^\top {}^{I k} \boldsymbol{\omega}) \\ \mathbf{H}_{tI} \end{bmatrix} \quad (111)$$

¹We assume that the two wheel encoders are hardware synchronized and thus their readings have the same timestamps.

$$\begin{aligned}
\mathbf{H}_{t1} = & \Lambda \left({}^O_I \hat{\mathbf{R}} \left[{}^G \hat{\mathbf{R}}^G \hat{\mathbf{p}}_{I_{k+1}} + {}^G \hat{\mathbf{R}}^G \hat{\mathbf{p}}_{I_{k+1}} + {}^G \hat{\mathbf{R}}^G \hat{\mathbf{p}}_{I_{k+1}} + {}^G \hat{\mathbf{R}}^G \hat{\mathbf{p}}_{I_{k+1}} \right]^{I_k} \boldsymbol{\omega} \right. \\
& \left. + {}^O_I \hat{\mathbf{R}}^G \hat{\mathbf{R}}^G \hat{\mathbf{v}}_{I_{k+1}} - {}^O_I \hat{\mathbf{R}}^G \hat{\mathbf{R}}^G \hat{\mathbf{v}}_{I_{k+1}} - {}^O_I \hat{\mathbf{R}}^G \hat{\mathbf{R}}^G \hat{\mathbf{v}}_{I_{k+1}} \right]^{I_{k+1}} \boldsymbol{\omega} - {}^O_I \hat{\mathbf{R}}^G \hat{\mathbf{R}}^G \hat{\mathbf{v}}_{I_k} \end{aligned} \quad (112)$$

2.4 Odometry Measurement Update

At this point, we have obtained the preintegrated wheel odometry measurements along with their corresponding Jacobians which are readily used for the MSCKF update:

$$\mathbf{z}_{k+1} := \mathbf{g}(\omega_{l(k:k+1)}, \omega_{r(k:k+1)}, \mathbf{x}_{WI}) = \mathbf{h}(\mathbf{x}_{I_{k+1}}, \mathbf{x}_{C_{k+1}}, \mathbf{x}_{WE}, {}^O t_I) \quad (113)$$

$$\approx \mathbf{g}(\omega_{ml(k:k+1)}, \omega_{mr(k:k+1)}, \hat{\mathbf{x}}_{WI}) + \frac{\partial \mathbf{g}}{\partial \tilde{\mathbf{x}}_{WI}} \tilde{\mathbf{x}}_{WI} + \frac{\partial \mathbf{g}}{\partial \mathbf{n}_\omega} \mathbf{n}_\omega \quad (114)$$

$$\approx \mathbf{h}(\hat{\mathbf{x}}_{I_{k+1}}, \hat{\mathbf{x}}_{C_{k+1}}, \hat{\mathbf{x}}_{WE}, {}^O \hat{t}_I) + \frac{\partial \mathbf{h}}{\partial \tilde{\mathbf{x}}_{I_{k+1}}} \tilde{\mathbf{x}}_{I_{k+1}} + \frac{\partial \mathbf{h}}{\partial \tilde{\mathbf{x}}_{C_{k+1}}} \tilde{\mathbf{x}}_{C_{k+1}} + \frac{\partial \mathbf{h}}{\partial \tilde{\mathbf{x}}_{WE}} \tilde{\mathbf{x}}_{WE} + \frac{\partial \mathbf{h}}{\partial {}^O \tilde{t}_I} {}^O \tilde{t}_I \quad (115)$$

$$\tilde{\mathbf{z}}_{k+1} := \mathbf{g}(\omega_{ml(k:k+1)}, \omega_{mr(k:k+1)}, \hat{\mathbf{x}}_{WI}) - \mathbf{h}(\hat{\mathbf{x}}_{I_{k+1}}, \hat{\mathbf{x}}_{C_{k+1}}, \hat{\mathbf{x}}_{WE}, {}^O \hat{t}_I) \quad (116)$$

$$\approx \underbrace{\left[\frac{\partial \mathbf{h}}{\partial \tilde{\mathbf{x}}_{I_{k+1}}} \quad \frac{\partial \mathbf{h}}{\partial \tilde{\mathbf{x}}_{C_{k+1}}} \quad \frac{\partial \mathbf{h}}{\partial \tilde{\mathbf{x}}_{WE}} \quad -\frac{\partial \mathbf{g}}{\partial \tilde{\mathbf{x}}_{WI}} \quad \frac{\partial \mathbf{g}}{\partial {}^O \tilde{t}_I} \right]}_{\mathbf{H}_{k+1}} \tilde{\mathbf{x}}_{k+1} - \frac{\partial \mathbf{g}}{\partial \mathbf{n}_\omega} \mathbf{n}_\omega \quad (117)$$

Note that similar to how we treat visual features, we also employ the Mahalanobis distance test to reject bad preintegrated odometry measurements (which can be due to some unmodelled errors such as slippage) and only those passing the χ^2 test will be used for EKF update.

3 Observability Analysis

As system observability plays an important role for state estimation [9, 4], we perform the observability analysis to gain insights about the state/parameter identifiability for the proposed VIWO.

For the analysis purpose, in analogy to [10], we consider the following state vector which includes a single cloned pose of $\mathbf{x}_{I_{k-1}}$ and a single 3D point feature ${}^G\mathbf{p}_f$:

$$\mathbf{x}_k = [\mathbf{x}_{I_k}^\top \quad \mathbf{x}_{C_k}^\top \quad \mathbf{x}_{WE}^\top \quad o_{t_I} \quad \mathbf{x}_{WI}^\top \quad {}^G\mathbf{p}_f^\top]^\top \quad (118)$$

The observability matrix for the linearized system is:

$$\mathbf{M} = \begin{bmatrix} \mathbf{H}_0 \\ \mathbf{H}_1 \Phi(t_1, t_0) \\ \vdots \\ \mathbf{H}_k \Phi(t_k, t_0) \\ \mathbf{H}_{k+1} \Phi(t_{k+1}, t_0) \\ \vdots \end{bmatrix} \quad (119)$$

where $\Phi(k, 0)$ is the state transition matrix which is not obvious when including the clone in the state vector and will be derived below, and \mathbf{H}_k is the stacked visual/wheel measurement Jacobian at time step k ((17),(18), and(117)). If we can find matrix \mathbf{N} that satisfies $\mathbf{M}\mathbf{N} = \mathbf{0}$, the basis of \mathbf{N} indicate the unobservable directions of the linearized system.

3.1 State Transition Matrix

In the MSCKF-based linearized system, the state transition matrix corresponding to the cloned state essentially reveals the stochastic cloning process. To see this, first recall how the cloned states are processed [11]: (i) augment the state with the current IMU pose when a new image is available, (ii) propagate the cloned pose with zero dynamics, (iii) marginalize the oldest clone after update if reaching the maximum size of the sliding window. In the case of one clone, this cloning process in respect to the error state corresponds to the following operation (while marginalization in the covariance form is trivial):

$$\tilde{\mathbf{x}}_{k|k} \leftarrow \begin{bmatrix} \mathbf{I}_3 & \mathbf{0}_3 & \mathbf{0}_3 & \mathbf{0}_3 & \mathbf{0}_3 & \mathbf{0}_3 & \mathbf{0}_3 & \mathbf{0}_{3 \times 13} \\ \mathbf{0}_3 & \mathbf{I}_3 & \mathbf{0}_3 & \mathbf{0}_3 & \mathbf{0}_3 & \mathbf{0}_3 & \mathbf{0}_3 & \mathbf{0}_{3 \times 13} \\ \mathbf{0}_3 & \mathbf{0}_3 & \mathbf{I}_3 & \mathbf{0}_3 & \mathbf{0}_3 & \mathbf{0}_3 & \mathbf{0}_3 & \mathbf{0}_{3 \times 13} \\ \mathbf{0}_3 & \mathbf{0}_3 & \mathbf{0}_3 & \mathbf{I}_3 & \mathbf{0}_3 & \mathbf{0}_3 & \mathbf{0}_3 & \mathbf{0}_{3 \times 13} \\ \mathbf{0}_3 & \mathbf{0}_3 & \mathbf{0}_3 & \mathbf{0}_3 & \mathbf{I}_3 & \mathbf{0}_3 & \mathbf{0}_3 & \mathbf{0}_{3 \times 13} \\ \mathbf{I}_3 & \mathbf{0}_3 & \mathbf{0}_3 & \mathbf{0}_3 & \mathbf{0}_3 & \mathbf{0}_3 & \mathbf{0}_3 & \mathbf{0}_{3 \times 13} \\ \mathbf{0}_3 & \mathbf{I}_3 & \mathbf{0}_3 & \mathbf{0}_3 & \mathbf{0}_3 & \mathbf{0}_3 & \mathbf{0}_3 & \mathbf{0}_{3 \times 13} \\ \mathbf{0}_{13 \times 3} & \mathbf{I}_{13} \end{bmatrix} \tilde{\mathbf{x}}_{k|k} \quad (120)$$

Note \mathbf{I}_3 at 6-th and 7-th row copy the IMU poses of the state to the clone state. One may model this state transition by including all the clones (with zero dynamics) in the state vector. This may complicate the analysis as it needs to explicitly include all the clone constraints, while we here construct the state transition matrix with implicit clone constraints.

We discover that cloning and propagating the current error state $\tilde{\mathbf{x}}_k$ can be unified by the following linear mapping:

$$\tilde{\mathbf{x}}_{k+1} = \underbrace{\begin{bmatrix} \Phi_{I_{11}}(t_{k+1}, t_k) & \mathbf{0}_3 & \mathbf{0}_3 & \Phi_{I_{14}}(t_{k+1}, t_k) & \mathbf{0}_3 & \mathbf{0}_3 & \mathbf{0}_3 & \mathbf{0}_{3 \times 13} \\ \Phi_{I_{21}}(t_{k+1}, t_k) & \mathbf{I}_3 & \Phi_{I_{23}}(t_{k+1}, t_k) & \Phi_{I_{24}}(t_{k+1}, t_k) & \Phi_{I_{25}}(t_{k+1}, t_k) & \mathbf{0}_3 & \mathbf{0}_3 & \mathbf{0}_{3 \times 13} \\ \Phi_{I_{31}}(t_{k+1}, t_k) & \mathbf{0}_3 & \mathbf{I}_3 & \Phi_{I_{34}}(t_{k+1}, t_k) & \Phi_{I_{35}}(t_{k+1}, t_k) & \mathbf{0}_3 & \mathbf{0}_3 & \mathbf{0}_{3 \times 13} \\ \mathbf{0}_3 & \mathbf{0}_3 & \mathbf{0}_3 & \mathbf{I}_3 & \mathbf{0}_3 & \mathbf{0}_3 & \mathbf{0}_3 & \mathbf{0}_{3 \times 13} \\ \mathbf{0}_3 & \mathbf{0}_3 & \mathbf{0}_3 & \mathbf{0}_3 & \mathbf{I}_3 & \mathbf{0}_3 & \mathbf{0}_3 & \mathbf{0}_{3 \times 13} \\ \mathbf{I}_3 & \mathbf{0}_3 & \mathbf{0}_3 & \mathbf{0}_3 & \mathbf{0}_3 & \mathbf{0}_3 & \mathbf{0}_3 & \mathbf{0}_{3 \times 13} \\ \mathbf{0}_3 & \mathbf{I}_3 & \mathbf{0}_3 & \mathbf{0}_3 & \mathbf{0}_3 & \mathbf{0}_3 & \mathbf{0}_3 & \mathbf{0}_{3 \times 13} \\ \mathbf{0}_{13 \times 3} & \mathbf{I}_{13} \end{bmatrix}}_{\Xi(k+1, k)} \tilde{\mathbf{x}}_k \quad (121)$$

where Φ_I is the error state transition matrix of IMU state [see (8)]. Note \mathbf{I}_3 at 6-th and 7-th row copy the IMU pose of $\tilde{\mathbf{x}}_k$ into $\tilde{\mathbf{x}}_{k+1}$ as a cloned pose without changing its value, while the cloned state in $\tilde{\mathbf{x}}_k$ has been discarded (marginalized). The above operation clearly reveals the MSCKF cloning process and thus, we will leverage this linear system (121) for the ensuing analysis.

Specifically, during the time interval $[t_0, t_{k+1}]$, we have the following linear dynamic system:

$$\tilde{\mathbf{x}}_{k+1} = \underbrace{\Xi(t_{k+1}, t_k) \Xi(t_k, t_{k-1}) \cdots \Xi(t_1, t_0)}_{\Xi(t_{k+1}, t_0)} \tilde{\mathbf{x}}_0 \quad (122)$$

$$\Xi(t_{k+1}, t_0) = \begin{bmatrix} \Phi_{I_{11}}(t_{k+1}, t_0) & \mathbf{0}_3 & \mathbf{0}_3 & \Phi_{I_{14}}(t_{k+1}, t_0) & \mathbf{0}_3 & \mathbf{0}_3 & \mathbf{0}_3 & \mathbf{0}_{3 \times 13} \\ \Phi_{I_{21}}(t_{k+1}, t_0) & \mathbf{I}_3 & \Phi_{I_{23}}(t_{k+1}, t_0) & \Phi_{I_{24}}(t_{k+1}, t_0) & \Phi_{I_{25}}(t_{k+1}, t_0) & \mathbf{0}_3 & \mathbf{0}_3 & \mathbf{0}_{3 \times 13} \\ \Phi_{I_{31}}(t_{k+1}, t_0) & \mathbf{0}_3 & \mathbf{I}_3 & \Phi_{I_{34}}(t_{k+1}, t_0) & \Phi_{I_{35}}(t_{k+1}, t_0) & \mathbf{0}_3 & \mathbf{0}_3 & \mathbf{0}_{3 \times 13} \\ \mathbf{0}_3 & \mathbf{0}_3 & \mathbf{0}_3 & \mathbf{I}_3 & \mathbf{0}_3 & \mathbf{0}_3 & \mathbf{0}_3 & \mathbf{0}_{3 \times 13} \\ \mathbf{0}_3 & \mathbf{0}_3 & \mathbf{0}_3 & \mathbf{0}_3 & \mathbf{I}_3 & \mathbf{0}_3 & \mathbf{0}_3 & \mathbf{0}_{3 \times 13} \\ \Psi_{C_{11}}(t_{k+1}, t_0) & \mathbf{0}_3 & \mathbf{0}_3 & \Psi_{C_{14}}(t_{k+1}, t_0) & \mathbf{0}_3 & \mathbf{0}_3 & \mathbf{0}_3 & \mathbf{0}_{3 \times 13} \\ \Psi_{C_{21}}(t_{k+1}, t_0) & \mathbf{I}_3 & \Psi_{C_{23}}(t_{k+1}, t_0) & \Psi_{C_{24}}(t_{k+1}, t_0) & \Psi_{C_{25}}(t_{k+1}, t_0) & \mathbf{0}_3 & \mathbf{0}_3 & \mathbf{0}_{3 \times 13} \\ \mathbf{0}_{13 \times 3} & \mathbf{I}_{13} \end{bmatrix} \quad (123)$$

$$\Psi_{C_{11}}(t_{k+1}, t_0) = \Phi_{I_{11}}(t_k, t_0) \quad (124)$$

$$\Psi_{C_{14}}(t_{k+1}, t_0) = \Phi_{I_{14}}(t_k, t_0) \quad (125)$$

$$\Psi_{C_{21}}(t_{k+1}, t_0) = \Phi_{I_{21}}(t_k, t_0) \quad (126)$$

$$\Psi_{C_{23}}(t_{k+1}, t_0) = \Phi_{I_{23}}(t_k, t_0) \quad (127)$$

$$\Psi_{C_{24}}(t_{k+1}, t_0) = \Phi_{I_{24}}(t_k, t_0) \quad (128)$$

$$\Psi_{C_{25}}(t_{k+1}, t_0) = \Phi_{I_{25}}(t_k, t_0) \quad (129)$$

The blue highlighted parts of the equations were derived incorrectly in the previous version of this documentation (found by Chuchu Chen). Though this error does not affect any of the observability analysis results followed by this chapter, we hereby note the mistake and show the correct derivation. Since the clone pose is the history of the IMU pose, we also enforce the constraint that the initial IMU pose and the clone state at time t_0 are identical as:

$$\begin{matrix} I_0 \\ G \end{matrix} \bar{\mathbf{q}} = \begin{matrix} I_{clone,0} \\ G \end{matrix} \bar{\mathbf{q}}, \quad \begin{matrix} G \\ \mathbf{P} \end{matrix} \mathbf{I}_0 = \begin{matrix} G \\ \mathbf{P} \end{matrix} \mathbf{I}_{clone,0} \quad (130)$$

where $\{\begin{matrix} I_{clone,0} \\ G \end{matrix} \bar{\mathbf{q}}, \begin{matrix} G \\ \mathbf{P} \end{matrix} \mathbf{I}_{clone,0}\}$ are the initial pose of the clone state. The above relation can be expressed as following geometrical constraints:

$$\begin{bmatrix} \mathbf{I}_4 & \mathbf{0}_{4 \times 12} & -\mathbf{I}_4 & \mathbf{0}_{4 \times 17} \end{bmatrix} \mathbf{x}_0 = \mathbf{0}_{4 \times 1} \quad (131)$$

$$\begin{bmatrix} \mathbf{0}_{3 \times 4} & \mathbf{I}_3 & \mathbf{0}_{3 \times 9} & \mathbf{0}_{3 \times 4} & -\mathbf{I}_3 & \mathbf{0}_{3 \times 14} \end{bmatrix} \mathbf{x}_0 = \mathbf{0}_{3 \times 1} \quad (132)$$

Through linearization, the constraint of the error states is:

$$\begin{bmatrix} \mathbf{I}_3 & \mathbf{0}_3 & \mathbf{0}_{3 \times 9} & -\mathbf{I}_3 & \mathbf{0}_3 & \mathbf{0}_{3 \times 13} \\ \mathbf{0}_3 & \mathbf{I}_3 & \mathbf{0}_{3 \times 9} & \mathbf{0}_3 & -\mathbf{I}_3 & \mathbf{0}_{3 \times 13} \end{bmatrix} \tilde{\mathbf{x}}_0 = \mathbf{0}_{6 \times 1} \quad (133)$$

With (133), we can convert the 6-th and 7-th row of (122) as:

$$\begin{bmatrix} I_{clone,k+1} \tilde{\boldsymbol{\theta}} \\ G \\ G \\ \tilde{\mathbf{p}}_{I_{clone,k+1}} \end{bmatrix} = \begin{bmatrix} \Psi_{C_{11}}(t_{k+1}, t_0) & \mathbf{0}_3 & \mathbf{0}_3 & \Psi_{C_{14}}(t_{k+1}, t_0) & \mathbf{0}_3 & \mathbf{0}_3 & \mathbf{0}_3 & \mathbf{0}_{3 \times 13} \\ \Psi_{C_{21}}(t_{k+1}, t_0) & \mathbf{I}_3 & \Psi_{C_{23}}(t_{k+1}, t_0) & \Psi_{C_{24}}(t_{k+1}, t_0) & \Psi_{C_{25}}(t_{k+1}, t_0) & \mathbf{0}_3 & \mathbf{0}_3 & \mathbf{0}_{3 \times 13} \end{bmatrix} \tilde{\mathbf{x}}_0 \quad (134)$$

$$= \begin{bmatrix} \Psi_{C_{11}}(t_{k+1}, t_0) I_G^0 \tilde{\boldsymbol{\theta}} + \Psi_{C_{14}}(t_{k+1}, t_0) \mathbf{b}_g \\ \Psi_{C_{21}}(t_{k+1}, t_0) I_G^0 \tilde{\boldsymbol{\theta}} + G \tilde{\mathbf{p}}_{I_0} + \Psi_{C_{23}}(t_{k+1}, t_0) G \tilde{\mathbf{v}}_{I_0} + \Psi_{C_{24}}(t_{k+1}, t_0) \mathbf{b}_g + \Psi_{C_{25}}(t_{k+1}, t_0) \mathbf{b}_a \end{bmatrix} \quad (135)$$

$$= \begin{bmatrix} \Psi_{C_{11}}(t_{k+1}, t_0) I_G^{I_{clone,0}} \tilde{\boldsymbol{\theta}} + \Psi_{C_{14}}(t_{k+1}, t_0) \mathbf{b}_g \\ \Psi_{C_{21}}(t_{k+1}, t_0) I_G^{I_{clone,0}} \tilde{\boldsymbol{\theta}} + G \tilde{\mathbf{p}}_{I_{clone,0}} + \Psi_{C_{23}}(t_{k+1}, t_0) G \tilde{\mathbf{v}}_{I_0} + \Psi_{C_{24}}(t_{k+1}, t_0) \mathbf{b}_g + \Psi_{C_{25}}(t_{k+1}, t_0) \mathbf{b}_a \end{bmatrix} \quad (136)$$

$$= \begin{bmatrix} \mathbf{0}_3 & \mathbf{0}_3 & \mathbf{0}_3 & \Psi_{C_{14}}(t_{k+1}, t_0) & \mathbf{0}_3 & \Psi_{C_{11}}(t_{k+1}, t_0) & \mathbf{0}_3 & \mathbf{0}_{3 \times 13} \\ \mathbf{0}_3 & \mathbf{0}_3 & \Psi_{C_{23}}(t_{k+1}, t_0) & \Psi_{C_{24}}(t_{k+1}, t_0) & \Psi_{C_{25}}(t_{k+1}, t_0) & \Psi_{C_{21}}(t_{k+1}, t_0) & \mathbf{I}_3 & \mathbf{0}_{3 \times 13} \end{bmatrix} \tilde{\mathbf{x}}_0 \quad (137)$$

We finally have the following state transition matrix $\Phi_{(t_{k+1}, t_0)}$ for our observability analysis:

$$\tilde{\mathbf{x}}_{k+1} = \underbrace{\begin{bmatrix} \Phi_{I_{11}}(t_{k+1}, t_0) & \mathbf{0}_3 & \mathbf{0}_3 & \Phi_{I_{14}}(t_{k+1}, t_0) & \mathbf{0}_3 & \mathbf{0}_3 & \mathbf{0}_3 & \mathbf{0}_{3 \times 13} \\ \Phi_{I_{21}}(t_{k+1}, t_0) & \mathbf{I}_3 & \Phi_{I_{23}}(t_{k+1}, t_0) & \Phi_{I_{24}}(t_{k+1}, t_0) & \Phi_{I_{25}}(t_{k+1}, t_0) & \mathbf{0}_3 & \mathbf{0}_3 & \mathbf{0}_{3 \times 13} \\ \Phi_{I_{31}}(t_{k+1}, t_0) & \mathbf{0}_3 & \mathbf{I}_3 & \Phi_{I_{34}}(t_{k+1}, t_0) & \Phi_{I_{35}}(t_{k+1}, t_0) & \mathbf{0}_3 & \mathbf{0}_3 & \mathbf{0}_{3 \times 13} \\ \mathbf{0}_3 & \mathbf{0}_3 & \mathbf{0}_3 & \mathbf{I}_3 & \mathbf{0}_3 & \mathbf{0}_3 & \mathbf{0}_3 & \mathbf{0}_{3 \times 13} \\ \mathbf{0}_3 & \mathbf{0}_3 & \mathbf{0}_3 & \mathbf{0}_3 & \mathbf{I}_3 & \mathbf{0}_3 & \mathbf{0}_3 & \mathbf{0}_{3 \times 13} \\ \mathbf{0}_3 & \mathbf{0}_3 & \mathbf{0}_3 & \Psi_{C_{14}}(t_{k+1}, t_0) & \mathbf{0}_3 & \Psi_{C_{11}}(t_{k+1}, t_0) & \mathbf{0}_3 & \mathbf{0}_{3 \times 13} \\ \mathbf{0}_3 & \mathbf{0}_3 & \Psi_{C_{23}}(t_{k+1}, t_0) & \Psi_{C_{24}}(t_{k+1}, t_0) & \Psi_{C_{25}}(t_{k+1}, t_0) & \Psi_{C_{21}}(t_{k+1}, t_0) & \mathbf{I}_3 & \mathbf{0}_{3 \times 13} \\ \mathbf{0}_{13 \times 3} & \mathbf{I}_{13} \end{bmatrix}}_{\Phi_{(t_{k+1}, t_0)}} \tilde{\mathbf{x}}_0 \quad (138)$$

3.2 Observability Properties

Based on the measurement Jacobians and state transition matrix [see (17), (18), (117) and (138)], we are able to construct the observability matrix (119) of the MSCKF-based linearized system under consideration. To be specific, the stacked Jacobian matrix of visual/wheel measurement \mathbf{H}_{k+1} at $k+2$ -th block row of the observability matrix has the following components:

$$\mathbf{H}_{k+1} = \begin{bmatrix} \mathbf{H}_{01} & \mathbf{H}_{02} & \mathbf{0}_{2 \times 9} & \mathbf{0}_{2 \times 3} & \mathbf{0}_{2 \times 3} & \mathbf{0}_{2 \times 3} & \mathbf{0}_{2 \times 3} & \mathbf{0}_{2 \times 1} & \mathbf{0}_{2 \times 1} & \mathbf{0}_{2 \times 1} & \mathbf{0}_{2 \times 1} & \mathbf{H}_{0e} \\ \mathbf{H}_{11} & \mathbf{0}_{1 \times 3} & \mathbf{0}_{1 \times 9} & \mathbf{H}_{16} & \mathbf{0}_{1 \times 3} & \mathbf{H}_{18} & \mathbf{0}_{1 \times 3} & \mathbf{H}_{1a} & \mathbf{H}_{1b} & \mathbf{H}_{1c} & \mathbf{H}_{1d} & \mathbf{0}_{1 \times 3} \\ \mathbf{H}_{21} & \mathbf{H}_{22} & \mathbf{0}_{2 \times 9} & \mathbf{H}_{26} & \mathbf{H}_{27} & \mathbf{H}_{28} & \mathbf{H}_{29} & \mathbf{H}_{2a} & \mathbf{H}_{2b} & \mathbf{H}_{2c} & \mathbf{H}_{2d} & \mathbf{0}_{2 \times 3} \end{bmatrix} \quad (139)$$

where

$$\mathbf{H}_{01} = \mathbf{H}_{pI}^C \hat{\mathbf{R}}_G^{I_{k+1}} \hat{\mathbf{R}} (G \hat{\mathbf{p}}_f - G \hat{\mathbf{p}}_{I_{k+1}}) \quad \mathbf{H}_{02} = -\mathbf{H}_{pI}^C \hat{\mathbf{R}}_G^{I_{k+1}} \hat{\mathbf{R}} \quad (140)$$

$$\mathbf{H}_{0e} = \mathbf{H}_{pI}^C \hat{\mathbf{R}}_G^{I_{k+1}} \hat{\mathbf{R}} \quad (141)$$

$$\mathbf{H}_{11} = \mathbf{e}_3^\top I_G^O \hat{\mathbf{R}} \quad \mathbf{H}_{16} = -\mathbf{e}_3^\top I_G^O \hat{\mathbf{R}}_G^{I_{k+1}} \hat{\mathbf{R}}_G^{I_k} \hat{\mathbf{R}}^\top \quad (142)$$

$$\mathbf{H}_{18} = \mathbf{e}_3^\top (\mathbf{I} - {}^O\hat{\mathbf{R}}_G^{I_{k+1}} \hat{\mathbf{R}}_G^{I_k} \hat{\mathbf{R}}^\top {}^O\hat{\mathbf{R}}^\top) \quad \mathbf{H}_{1a} = \mathbf{e}_3^\top {}^O\hat{\mathbf{R}}^{(I_{k+1}\boldsymbol{\omega} - {}^G\hat{\mathbf{R}}_G^{I_k} \hat{\mathbf{R}}^\top I_k \boldsymbol{\omega})} \quad (143)$$

$$\mathbf{H}_{1b} = \sum_{i=1}^n \Delta t_i \frac{\omega_{ml,i}}{\hat{b}} \quad \mathbf{H}_{1c} = \sum_{i=1}^n -\Delta t_i \frac{\omega_{mr,i}}{\hat{b}} \quad (144)$$

$$\mathbf{H}_{1d} = \sum_{i=1}^n \Delta t_i \frac{\omega_{mr,i} \hat{r}_r - \omega_{ml,i} \hat{r}_l}{\hat{b}^2} \quad (145)$$

$$\mathbf{H}_{21} = -\Lambda_I^O \hat{\mathbf{R}}_G^{I_k} \hat{\mathbf{R}}_G^{I_{k+1}} \hat{\mathbf{R}}^\top [I \hat{\mathbf{p}}_O] \quad \mathbf{H}_{22} = \Lambda_I^O \hat{\mathbf{R}}_G^{I_k} \hat{\mathbf{R}} \quad (146)$$

$$\mathbf{H}_{26} = \Lambda_I^O \hat{\mathbf{R}}_G^{I_k} \hat{\mathbf{R}} ({}^G\hat{\mathbf{p}}_{I_{k+1}} + {}^G\hat{\mathbf{R}}^{I_{k+1}} \hat{\mathbf{R}}^\top I \hat{\mathbf{p}}_O - {}^G\hat{\mathbf{p}}_{I_k}) \quad \mathbf{H}_{27} = -\Lambda_I^O \hat{\mathbf{R}}_G^{I_k} \hat{\mathbf{R}} \quad (147)$$

$$\mathbf{H}_{28} = \Lambda(({}^O\hat{\mathbf{R}}_G^{I_k} \hat{\mathbf{R}} ({}^G\hat{\mathbf{p}}_{I_{k+1}} + {}^G\hat{\mathbf{R}}^{I_{k+1}} \hat{\mathbf{R}}^\top I \hat{\mathbf{p}}_O - {}^G\hat{\mathbf{p}}_{I_k})) + {}^O\hat{\mathbf{R}}_G^{I_k} \hat{\mathbf{R}}_G^{I_{k+1}} \hat{\mathbf{R}}^\top {}^O\hat{\mathbf{R}}^\top [{}^O\hat{\mathbf{p}}_I]) \quad (148)$$

$$\mathbf{H}_{29} = \Lambda(\mathbf{I} - {}^O\hat{\mathbf{R}}_G^{I_k} \hat{\mathbf{R}}_G^{I_{k+1}} \hat{\mathbf{R}}^\top {}^O\hat{\mathbf{R}}^\top) \quad (149)$$

$$\begin{aligned} \mathbf{H}_{2a} = & \Lambda({}^O\hat{\mathbf{R}}_G^{I_k} \hat{\mathbf{R}}_G^{I_{k+1}} \hat{\mathbf{R}}^\top I \hat{\mathbf{p}}_O - {}^G\hat{\mathbf{R}}_G^{I_k} \hat{\mathbf{R}}^\top I \hat{\mathbf{p}}_O - {}^G\hat{\mathbf{p}}_{I_k}) I_k \boldsymbol{\omega} \\ & + {}^O\hat{\mathbf{R}}_G^{I_k} \hat{\mathbf{R}}_G^{I_{k+1}} \hat{\mathbf{R}}^\top I \hat{\mathbf{p}}_O - {}^G\hat{\mathbf{R}}_G^{I_k} \hat{\mathbf{R}}_G^{I_{k+1}} \hat{\mathbf{R}}^\top [I \hat{\mathbf{p}}_O] I_{k+1} \boldsymbol{\omega} - {}^O\hat{\mathbf{R}}_G^{I_k} \hat{\mathbf{R}}_G^{I_{k+1}} \hat{\mathbf{R}}^\top \hat{\mathbf{v}}_{I_k} \end{aligned} \quad (150)$$

$$\mathbf{H}_{2b} = \begin{bmatrix} \sum_{i=1}^n h_{x\omega,i} \frac{\omega_{ml,i}}{\hat{b}} - h_{xv,i} \frac{\omega_{ml,i}}{2} + h_{x\theta,i} \sum_{j=1}^{i-1} \Delta t_j \frac{\omega_{ml,j}}{\hat{b}} \\ \sum_{i=1}^n h_{y\omega,i} \frac{\omega_{ml,i}}{\hat{b}} - h_{yv,i} \frac{\omega_{ml,i}}{2} + h_{y\theta,i} \sum_{j=1}^{i-1} \Delta t_j \frac{\omega_{ml,j}}{\hat{b}} \end{bmatrix} \quad (151)$$

$$\mathbf{H}_{2c} = \begin{bmatrix} \sum_{i=1}^n -h_{x\omega,i} \frac{\omega_{mr,i}}{\hat{b}} - h_{xv,i} \frac{\omega_{mr,i}}{2} - h_{x\theta,i} \sum_{j=1}^{i-1} \Delta t_j \frac{\omega_{mr,j}}{\hat{b}} \\ \sum_{i=1}^n -h_{y\omega,i} \frac{\omega_{mr,i}}{\hat{b}} - h_{yv,i} \frac{\omega_{mr,i}}{2} - h_{y\theta,i} \sum_{j=1}^{i-1} \Delta t_j \frac{\omega_{mr,j}}{\hat{b}} \end{bmatrix} \quad (152)$$

$$\mathbf{H}_{2d} = \begin{bmatrix} \sum_{i=1}^n h_{x\omega,i} \frac{\omega_{mr,i} \hat{r}_r - \omega_{ml,i} \hat{r}_l}{\hat{b}^2} + h_{x\theta,i} \sum_{j=1}^{i-1} \Delta t_j \frac{\omega_{mr,j} \hat{r}_r - \omega_{ml,j} \hat{r}_l}{\hat{b}^2} \\ \sum_{i=1}^n h_{y\omega,i} \frac{\omega_{mr,i} \hat{r}_r - \omega_{ml,i} \hat{r}_l}{\hat{b}^2} + h_{y\theta,i} \sum_{j=1}^{i-1} \Delta t_j \frac{\omega_{mr,j} \hat{r}_r - \omega_{ml,j} \hat{r}_l}{\hat{b}^2} \end{bmatrix} \quad (153)$$

Now, the $k+2$ -th block row of the observability matrix is:

$$\begin{aligned} \mathbf{M}_{k+2} &= \mathbf{H}_{k+1} \boldsymbol{\Phi}(t_{k+1}, t_0) \\ &= \begin{bmatrix} \boldsymbol{\Gamma}_0 \\ \boldsymbol{\Gamma}_1 \\ \boldsymbol{\Gamma}_2 \end{bmatrix} = \begin{bmatrix} \boldsymbol{\Gamma}_{01} & \boldsymbol{\Gamma}_{02} & \boldsymbol{\Gamma}_{03} & \boldsymbol{\Gamma}_{04} & \boldsymbol{\Gamma}_{05} & \mathbf{0}_{2 \times 3} & \mathbf{0}_{2 \times 3} & \mathbf{0}_{2 \times 3} & \mathbf{0}_{2 \times 3} & \mathbf{0}_{2 \times 1} & \mathbf{0}_{2 \times 1} & \mathbf{0}_{2 \times 1} & \mathbf{0}_{2 \times 1} & \boldsymbol{\Gamma}_{0e} \\ \boldsymbol{\Gamma}_{11} & \mathbf{0}_{1 \times 3} & \mathbf{0}_{1 \times 3} & \boldsymbol{\Gamma}_{14} & \mathbf{0}_{1 \times 3} & \boldsymbol{\Gamma}_{16} & \mathbf{0}_{1 \times 3} & \boldsymbol{\Gamma}_{18} & \mathbf{0}_{1 \times 3} & \boldsymbol{\Gamma}_{1a} & \boldsymbol{\Gamma}_{1b} & \boldsymbol{\Gamma}_{1c} & \boldsymbol{\Gamma}_{1d} & \mathbf{0}_{1 \times 3} \\ \boldsymbol{\Gamma}_{21} & \boldsymbol{\Gamma}_{22} & \boldsymbol{\Gamma}_{23} & \boldsymbol{\Gamma}_{24} & \boldsymbol{\Gamma}_{25} & \boldsymbol{\Gamma}_{26} & \boldsymbol{\Gamma}_{27} & \boldsymbol{\Gamma}_{28} & \boldsymbol{\Gamma}_{29} & \boldsymbol{\Gamma}_{2a} & \boldsymbol{\Gamma}_{2b} & \boldsymbol{\Gamma}_{2c} & \boldsymbol{\Gamma}_{2d} & \mathbf{0}_{2 \times 3} \end{bmatrix} \end{aligned} \quad (154)$$

where

$$\begin{array}{lll} \boldsymbol{\Gamma}_{01} = \mathbf{H}_{01} \boldsymbol{\Phi}_{11} + \mathbf{H}_{02} \boldsymbol{\Phi}_{21} & \boldsymbol{\Gamma}_{02} = \mathbf{H}_{02} & \boldsymbol{\Gamma}_{03} = \mathbf{H}_{02} \boldsymbol{\Phi}_{23} \\ \boldsymbol{\Gamma}_{04} = \mathbf{H}_{01} \boldsymbol{\Phi}_{14} + \mathbf{H}_{02} \boldsymbol{\Phi}_{24} & \boldsymbol{\Gamma}_{05} = \mathbf{H}_{02} \boldsymbol{\Phi}_{25} & \boldsymbol{\Gamma}_{0e} = \mathbf{H}_{0e} \\ \boldsymbol{\Gamma}_{11} = \mathbf{H}_{11} \boldsymbol{\Phi}_{11} & \boldsymbol{\Gamma}_{14} = \mathbf{H}_{11} \boldsymbol{\Phi}_{14} + \mathbf{H}_{16} \boldsymbol{\Phi}_{64} & \boldsymbol{\Gamma}_{16} = \mathbf{H}_{16} \boldsymbol{\Phi}_{66} \\ \boldsymbol{\Gamma}_{18} = \mathbf{H}_{18} & \boldsymbol{\Gamma}_{1a} = \mathbf{H}_{1a} & \boldsymbol{\Gamma}_{1b} = \mathbf{H}_{1b} \\ \boldsymbol{\Gamma}_{1c} = \mathbf{H}_{1c} & \boldsymbol{\Gamma}_{1d} = \mathbf{H}_{1d} & \boldsymbol{\Gamma}_{21} = \mathbf{H}_{21} \boldsymbol{\Phi}_{11} + \mathbf{H}_{22} \boldsymbol{\Phi}_{21} \\ \boldsymbol{\Gamma}_{22} = \mathbf{H}_{22} & \boldsymbol{\Gamma}_{23} = \mathbf{H}_{22} \boldsymbol{\Phi}_{23} + \mathbf{H}_{27} \boldsymbol{\Phi}_{73} & \boldsymbol{\Gamma}_{24} = \mathbf{H}_{21} \boldsymbol{\Phi}_{14} + \mathbf{H}_{22} \boldsymbol{\Phi}_{24} + \mathbf{H}_{26} \boldsymbol{\Phi}_{64} + \mathbf{H}_{72} \boldsymbol{\Phi}_{74} \\ \boldsymbol{\Gamma}_{25} = \mathbf{H}_{22} \boldsymbol{\Phi}_{25} + \mathbf{H}_{27} \boldsymbol{\Phi}_{75} & \boldsymbol{\Gamma}_{26} = \mathbf{H}_{26} \boldsymbol{\Phi}_{66} + \mathbf{H}_{27} \boldsymbol{\Phi}_{76} & \boldsymbol{\Gamma}_{27} = \mathbf{H}_{27} \\ \boldsymbol{\Gamma}_{28} = \mathbf{H}_{28} & \boldsymbol{\Gamma}_{29} = \mathbf{H}_{29} & \boldsymbol{\Gamma}_{2a} = \mathbf{H}_{2a} \\ \boldsymbol{\Gamma}_{2b} = \mathbf{H}_{2b} & \boldsymbol{\Gamma}_{2c} = \mathbf{H}_{2c} & \boldsymbol{\Gamma}_{2d} = \mathbf{H}_{2d} \end{array}$$

$\boldsymbol{\Phi}_{ij}$ are the block matrix of (138) at i -th row and j -th column.

Based on the observability matrix (119), the proposed VIWO has the following observability properties:

Lemma 3.1. *With general motions, there are four unobservable directions corresponding to the global position and the yaw angle as in VINS [10].*

Proof. The 4 unobservable directions of VINS corresponding to the state (118) is:

$$\mathbf{N}_{vins} = [\mathbf{N}_{vins_1} \quad \mathbf{N}_{vins_2}] = \begin{bmatrix} \mathbf{0}_3 & I_0 \mathbf{R} \mathbf{g} \\ \mathbf{I}_3 & -[{}^G \hat{\mathbf{p}}_{I_0}] \mathbf{g} \\ \mathbf{0}_3 & -[{}^G \hat{\mathbf{v}}_{I_0}] \mathbf{g} \\ \mathbf{0}_3 & \mathbf{0}_{3 \times 1} \\ \mathbf{0}_3 & \mathbf{0}_{3 \times 1} \\ \mathbf{0}_3 & I_0 \mathbf{R} \mathbf{g} \\ \mathbf{I}_3 & -[{}^G \hat{\mathbf{p}}_{I_0}] \mathbf{g} \\ \mathbf{0}_{10 \times 3} & \mathbf{0}_{10 \times 1} \\ \mathbf{I}_3 & -[{}^G \mathbf{p}_f] \mathbf{g} \end{bmatrix} \quad (155)$$

\mathbf{N}_{vins} is the null space of \mathbf{M}_{k+2} proving the unobservability of the 4 directions.

$$\mathbf{M}_{k+2} \mathbf{N}_{vins} = \begin{bmatrix} \mathbf{\Gamma}_0 \mathbf{N}_{vins_1} & \mathbf{\Gamma}_0 \mathbf{N}_{vins_2} \\ \mathbf{\Gamma}_1 \mathbf{N}_{vins_1} & \mathbf{\Gamma}_1 \mathbf{N}_{vins_2} \\ \mathbf{\Gamma}_2 \mathbf{N}_{vins_1} & \mathbf{\Gamma}_2 \mathbf{N}_{vins_2} \end{bmatrix} = \mathbf{0}_{5 \times 4} \quad (156)$$

This completes the proof. \square

Lemma 3.2. *If the system undergoes pure translation (no rotation), the translation part $O_{\mathbf{p}_I}$ of the spatial calibration and the baselink length b will be unobservable, with unobservable directions as:*

$$\mathbf{N}_{trans} = [\mathbf{N}_{trans_1} \quad \mathbf{N}_{trans_2}] = \begin{bmatrix} \mathbf{0}_{21 \times 3} & \mathbf{0}_{21 \times 1} \\ \mathbf{0}_3 & \mathbf{0}_{3 \times 1} \\ \mathbf{I}_3 & \mathbf{0}_{3 \times 1} \\ \mathbf{0}_{1 \times 3} & 0 \\ \mathbf{0}_{1 \times 3} & 0 \\ \mathbf{0}_{1 \times 3} & 0 \\ \mathbf{0}_{1 \times 3} & 1 \\ \mathbf{0}_3 & \mathbf{0}_{3 \times 1} \end{bmatrix} \quad (157)$$

Proof. Since the system undergoes pure translation, we have the following geometric constraints:

$${}^G \mathbf{R}^{I_{k+1}} = {}^G \mathbf{R}^{I_k} = {}^G \mathbf{R} \quad (158)$$

$$O_i \omega = \frac{\omega_{r,i} \hat{r}_r - \omega_{l,i} \hat{r}_l}{b} = 0 \quad \text{for } i \in 1, 2, \dots, n \quad (159)$$

By applying the above constraints, \mathbf{N}_{trans} become the null space of the observability matrix \mathbf{M}_{k+2} :

$$\mathbf{M}_{k+2} \mathbf{N}_{trans} = \begin{bmatrix} \mathbf{0}_{2 \times 3} & \mathbf{0}_{2 \times 1} \\ \mathbf{0}_{1 \times 3} & \mathbf{\Gamma}_{1d} \\ \mathbf{\Gamma}_{29} & \mathbf{\Gamma}_{2d} \end{bmatrix} \quad (160)$$

$$= \begin{bmatrix} \mathbf{0}_{2 \times 3} & \mathbf{0}_{2 \times 1} \\ \mathbf{0}_{1 \times 3} & \sum_{i=1}^n \Delta t_i \frac{\omega_{mr,i} \hat{r}_r - \omega_{ml,i} \hat{r}_l}{\hat{b}^2} \\ \Lambda (\mathbf{I} - O_I \hat{\mathbf{R}}_G^{I_k} \hat{\mathbf{R}}_G^{I_{k+1}} \hat{\mathbf{R}}^T O_I \hat{\mathbf{R}}^T) \begin{bmatrix} \sum_{i=1}^n h_{x\omega,i} \frac{\omega_{mr,i} \hat{r}_r - \omega_{ml,i} \hat{r}_l}{\hat{b}^2} + h_{x\theta,i} \sum_{j=1}^{i-1} \Delta t_j \frac{\omega_{mr,j} \hat{r}_r - \omega_{ml,j} \hat{r}_l}{\hat{b}^2} \\ \sum_{i=1}^n h_{y\omega,i} \frac{\omega_{mr,i} \hat{r}_r - \omega_{ml,i} \hat{r}_l}{\hat{b}^2} + h_{y\theta,i} \sum_{j=1}^{i-1} \Delta t_j \frac{\omega_{mr,j} \hat{r}_r - \omega_{ml,j} \hat{r}_l}{\hat{b}^2} \end{bmatrix} \end{bmatrix} \quad (161)$$

$$= \mathbf{0}_{5 \times 4} \quad (162)$$

This completes the proof. \square

Lemma 3.3. *If the system undergoes random (general) translation but with only one-axis IMU rotation, the translation calibration parameter ${}^O\mathbf{p}_I$ along the rotation axis will be unobservable, with the following unobservable direction:*

$$\mathbf{N}_{rot} = \begin{bmatrix} \mathbf{0}_{24 \times 1} \\ {}^O\hat{\mathbf{R}}\mathbf{u} \\ \mathbf{0}_{7 \times 1} \end{bmatrix} \quad (163)$$

where \mathbf{u} is the constant rotation axis in the IMU frame.

Proof. Since the system undergoes one-axis IMU rotation, we have the following geometric constraints:

$${}^{I_{k+1}}\mathbf{R}\mathbf{u} = {}^{I_k}\mathbf{R}\mathbf{u} = {}^{I_0}\mathbf{R}\mathbf{u} \quad (164)$$

By applying the above constraints, \mathbf{N}_{rot} become the null space of the observability matrix \mathbf{M}_{k+2} :

$$\mathbf{M}_{k+2}\mathbf{N}_{rot} = \begin{bmatrix} \mathbf{0}_{2 \times 3} \\ \mathbf{0}_{1 \times 3} \\ \mathbf{\Gamma}_{29} {}^O\hat{\mathbf{R}}\mathbf{u} \end{bmatrix} \quad (165)$$

$$= \begin{bmatrix} \mathbf{0}_{2 \times 3} \\ \mathbf{0}_{1 \times 3} \\ \Lambda(\mathbf{I} - {}^O\hat{\mathbf{R}}_G {}^{I_k}\hat{\mathbf{R}}_G {}^{I_{k+1}}\hat{\mathbf{R}}^{\top} {}^O\hat{\mathbf{R}}^{\top}) {}^O\hat{\mathbf{R}}\mathbf{u} \end{bmatrix} \quad (166)$$

$$= \mathbf{0}_{5 \times 4} \quad (167)$$

This completes the proof. \square

Lemma 3.4. *If the system undergoes constant local IMU angular velocity ${}^I\boldsymbol{\omega}$ and linear velocity ${}^I\mathbf{v}$, the time offset ${}^O t_I$ will be unobservable with the following unobservable direction:*

$$\mathbf{N}_{constv} = \begin{bmatrix} \mathbf{0}_{21 \times 1} \\ -{}^O\hat{\mathbf{R}} {}^{I_0}\boldsymbol{\omega} \\ {}^O\hat{\mathbf{R}} {}^{I_0}\mathbf{v} \\ 1 \\ \mathbf{0}_{6 \times 1} \end{bmatrix} \quad (168)$$

Proof. Since the system undergoes constant local IMU angular velocity ${}^I\boldsymbol{\omega}$ and linear velocity ${}^I\mathbf{v}$, we have the following geometric constraints:

$${}^{I_{k+1}}\boldsymbol{\omega} = {}^{I_k}\boldsymbol{\omega} = {}^{I_0}\boldsymbol{\omega} \quad (169)$$

$${}^{I_{k+1}}\mathbf{v} = {}^{I_k}\mathbf{v} = {}^{I_0}\mathbf{v} \quad (170)$$

By applying the above constraints, \mathbf{N}_{constv} become the null space of the observability matrix \mathbf{M}_{k+2} :

$$\mathbf{M}_{k+2}\mathbf{N}_{constv} = \begin{bmatrix} \mathbf{0}_{2 \times 3} \\ -\mathbf{\Gamma}_{18} {}^O\hat{\mathbf{R}} {}^{I_0}\boldsymbol{\omega} + \mathbf{\Gamma}_{1a} \\ -\mathbf{\Gamma}_{28} {}^O\hat{\mathbf{R}} {}^{I_0}\boldsymbol{\omega} + \mathbf{\Gamma}_{29} {}^O\hat{\mathbf{R}} {}^{I_0}\mathbf{v} + \mathbf{\Gamma}_{2a} \end{bmatrix} \quad (171)$$

$$= \begin{bmatrix} \mathbf{0}_{2 \times 3} \\ -\mathbf{e}_3^{\top}(\mathbf{I} - {}^O\hat{\mathbf{R}}_G {}^{I_{k+1}}\hat{\mathbf{R}}_G {}^{I_k}\hat{\mathbf{R}}^{\top} {}^O\hat{\mathbf{R}}^{\top}) {}^O\hat{\mathbf{R}} {}^{I_0}\boldsymbol{\omega} + \mathbf{e}_3^{\top} {}^O\hat{\mathbf{R}} ({}^{I_{k+1}}\boldsymbol{\omega} - {}^{I_{k+1}}\hat{\mathbf{R}}_G {}^{I_k}\hat{\mathbf{R}}^{\top} {}^{I_k}\boldsymbol{\omega}) \\ \mathbf{MN}_1 \end{bmatrix} \quad (172)$$

$$\begin{aligned}
&= \mathbf{0}_{5 \times 4} \tag{173} \\
\mathbf{MN}_1 &= -\Lambda([\mathop{O}_I \hat{\mathbf{R}}_G^{I_k} \hat{\mathbf{R}}_G^{I_{k+1}} \hat{\mathbf{p}}_{I_{k+1}} + \mathop{I}_{k+1} \hat{\mathbf{R}}^\top \hat{\mathbf{p}}_O - \mathop{G} \hat{\mathbf{p}}_{I_k}]) + \mathop{O}_I \hat{\mathbf{R}}_G^{I_k} \hat{\mathbf{R}}_G^{I_{k+1}} \hat{\mathbf{R}}^\top \mathop{O}_I \hat{\mathbf{R}}^\top [\mathop{O} \hat{\mathbf{p}}_I]) \mathop{O}_I \hat{\mathbf{R}}^{I_0} \boldsymbol{\omega} \\
&\Lambda(\mathbf{I} - \mathop{O}_I \hat{\mathbf{R}}_G^{I_k} \hat{\mathbf{R}}_G^{I_{k+1}} \hat{\mathbf{R}}^\top \mathop{O}_I \hat{\mathbf{R}}^\top) \mathop{O}_I \hat{\mathbf{R}}^{I_0} \mathbf{v} + \Lambda(\mathop{O}_I \hat{\mathbf{R}}_G^{I_k} \hat{\mathbf{R}}_G^{I_{k+1}} \hat{\mathbf{p}}_{I_{k+1}} + \mathop{I}_{k+1} \hat{\mathbf{R}}^\top \hat{\mathbf{p}}_O - \mathop{G} \hat{\mathbf{R}}_G^{I_k} \hat{\mathbf{p}}_{I_k}) \mathop{I}_{k+1} \boldsymbol{\omega} \\
&+ \mathop{O}_I \hat{\mathbf{R}}_G^{I_k} \hat{\mathbf{R}}_G^{I_{k+1}} \hat{\mathbf{v}}_{I_{k+1}} - \mathop{O}_I \hat{\mathbf{R}}_G^{I_k} \hat{\mathbf{R}}_G^{I_{k+1}} \hat{\mathbf{R}}^\top [\mathop{I} \hat{\mathbf{p}}_O] \mathop{I}_{k+1} \boldsymbol{\omega} - \mathop{O}_I \hat{\mathbf{R}}_G^{I_k} \hat{\mathbf{R}}_G^{I_{k+1}} \hat{\mathbf{v}}_{I_k} \tag{174}
\end{aligned}$$

This completes the proof. \square

Lemma 3.5. *If the system undergoes motions that does not execute left/right wheel movement, the intrinsic parameter r_l/r_r will be unobservable, with the following unobservable direction:*

$$\mathbf{N}_{radii} = \begin{bmatrix} \mathbf{0}_{28 \times 1} \\ 1 \\ 0 \\ \mathbf{0}_{4 \times 1} \end{bmatrix} \text{ or } \begin{bmatrix} \mathbf{0}_{28 \times 1} \\ 0 \\ 1 \\ \mathbf{0}_{4 \times 1} \end{bmatrix} \tag{175}$$

Proof. Since the system undergoes motions that does not execute left/right wheel movement, we have the following geometric constraints:

$$\omega_{l,i} = 0 \text{ or } \omega_{r,i} = 0 \text{ for } i \in 1, 2, \dots, n \tag{176}$$

By applying the above constraints, \mathbf{N}_{radii} become the null space of the observability matrix \mathbf{M}_{k+2} :

$$\mathbf{M}_{k+2} \mathbf{N}_{radii} = \begin{bmatrix} \mathbf{0}_{2 \times 3} \\ \boldsymbol{\Gamma}_{1b} \\ \boldsymbol{\Gamma}_{2b} \end{bmatrix} \text{ or } \begin{bmatrix} \mathbf{0}_{2 \times 3} \\ \boldsymbol{\Gamma}_{1c} \\ \boldsymbol{\Gamma}_{2c} \end{bmatrix} \tag{177}$$

$$\begin{aligned}
&= \begin{bmatrix} \mathbf{0}_{2 \times 3} \\ \sum_{i=1}^n \Delta t_i \frac{\omega_{ml,i}}{b} \\ \left[\begin{array}{c} \sum_{i=1}^n h_{x\omega,i} \frac{\omega_{ml,i}}{b} - h_{xv,i} \frac{\omega_{ml,i}}{2} + h_{x\theta,i} \sum_{j=1}^{i-1} \Delta t_j \frac{\omega_{ml,j}}{b} \\ \sum_{i=1}^n h_{y\omega,i} \frac{\omega_{ml,i}}{b} - h_{yv,i} \frac{\omega_{ml,i}}{2} + h_{y\theta,i} \sum_{j=1}^{i-1} \Delta t_j \frac{\omega_{ml,j}}{b} \end{array} \right] \end{bmatrix} \\
\text{or} & \begin{bmatrix} \mathbf{0}_{2 \times 3} \\ \sum_{i=1}^n -\Delta t_i \frac{\omega_{mr,i}}{b} \\ \left[\begin{array}{c} \sum_{i=1}^n -h_{x\omega,i} \frac{\omega_{mr,i}}{b} - h_{xv,i} \frac{\omega_{mr,i}}{2} - h_{x\theta,i} \sum_{j=1}^{i-1} \Delta t_j \frac{\omega_{mr,j}}{b} \\ \sum_{i=1}^n -h_{y\omega,i} \frac{\omega_{mr,i}}{b} - h_{yv,i} \frac{\omega_{mr,i}}{2} - h_{y\theta,i} \sum_{j=1}^{i-1} \Delta t_j \frac{\omega_{mr,j}}{b} \end{array} \right] \end{bmatrix} \tag{178}
\end{aligned}$$

$$= \mathbf{0}_{5 \times 4} \tag{179}$$

This completes the proof. \square

Lemma 3.6. *If the system does not move, all the calibration parameters ($\mathop{O}_I \mathbf{R}$, $\mathop{O}_{\mathbf{p}I}$, \mathop{O}_{I_1} , r_l , r_r , b)*

are unobservable, with the following unobservable direction:

$$\mathbf{N}_{no} = \begin{bmatrix} \mathbf{0}_{21 \times 3} & \mathbf{0}_{21 \times 3} & \mathbf{0}_{21 \times 1} & \mathbf{0}_{21 \times 1} & \mathbf{0}_{21 \times 1} & \mathbf{0}_{21 \times 1} \\ \mathbf{I}_3 & \mathbf{0}_3 & \mathbf{0}_{3 \times 1} & \mathbf{0}_{3 \times 1} & \mathbf{0}_{3 \times 1} & \mathbf{0}_{3 \times 1} \\ \mathbf{0}_3 & \mathbf{I}_3 & \mathbf{0}_{3 \times 1} & \mathbf{0}_{3 \times 1} & \mathbf{0}_{3 \times 1} & \mathbf{0}_{3 \times 1} \\ \mathbf{0}_{1 \times 3} & \mathbf{0}_{1 \times 3} & 1 & 0 & 0 & 0 \\ \mathbf{0}_{1 \times 3} & \mathbf{0}_{1 \times 3} & 0 & 1 & 0 & 0 \\ \mathbf{0}_{1 \times 3} & \mathbf{0}_{1 \times 3} & 0 & 0 & 1 & 0 \\ \mathbf{0}_{1 \times 3} & \mathbf{0}_{1 \times 3} & 0 & 0 & 0 & 1 \\ \mathbf{0}_3 & \mathbf{0}_3 & \mathbf{0}_{3 \times 1} & \mathbf{0}_{3 \times 1} & \mathbf{0}_{3 \times 1} & \mathbf{0}_{3 \times 1} \end{bmatrix} \quad (180)$$

Proof. Since the system does not move, we have the following geometric constraints:

$${}^G \mathbf{v}_{I_{k+1}} = {}^G \mathbf{v}_{I_k} = {}^G \mathbf{v}_{I_0} = \mathbf{0} \quad (181)$$

$$\boldsymbol{\omega}_{k+1} = \boldsymbol{\omega}_k = \boldsymbol{\omega}_0 = \mathbf{0} \quad (182)$$

$$\mathbf{a}_{k+1} = \mathbf{a}_k = \mathbf{a}_0 = \mathbf{0} \quad (183)$$

$${}^{I_{k+1}} \mathbf{R} = {}^{I_k} \mathbf{R} = {}^{I_0} \mathbf{R} \quad (184)$$

$${}^G \mathbf{p}_{I_{k+1}} = {}^G \mathbf{p}_{I_k} = {}^G \mathbf{p}_{I_0} \quad (185)$$

$$\omega_{r,i} = \omega_{l,i} = 0 \quad \text{for } i \in 1, 2, \dots, n \quad (186)$$

By applying the above constraints, \mathbf{N}_{no} become the null space of the observability matrix \mathbf{M}_{k+2} :

$$\mathbf{M}_{k+2} \mathbf{N}_{no} = \mathbf{0}_{5 \times 4} \quad (187)$$

This completes the proof. □

References

- [1] Anastasios I Mourikis and Stergios I Roumeliotis. “A multi-state constraint Kalman filter for vision-aided inertial navigation”. In: *Proceedings 2007 IEEE International Conference on Robotics and Automation*. IEEE. 2007, pp. 3565–3572.
- [2] Nikolas Trawny and Stergios I. Roumeliotis. *Indirect Kalman Filter for 3D Attitude Estimation*. Tech. rep. University of Minnesota, Dept. of Comp. Sci. & Eng., Mar. 2005.
- [3] Christoph Hertzberg et al. “Integrating generic sensor fusion algorithms with sound state representations through encapsulation of manifolds”. In: *Information Fusion* 14.1 (2013), pp. 57–77.
- [4] Joel A Hesch et al. “Observability-constrained vision-aided inertial navigation”. In: (2012).
- [5] Mingyang Li. “Visual-Inertial Odometry on Resource-Constrained Systems”. PhD thesis. UC Riverside, 2014.
- [6] Roland Siegwart, Illah Reza Nourbakhsh, and Davide Scaramuzza. *Introduction to autonomous mobile robots*. MIT press, 2011.
- [7] Kejian J Wu et al. “Vins on wheels”. In: *2017 IEEE International Conference on Robotics and Automation (ICRA)*. IEEE. 2017, pp. 5155–5162.
- [8] Gregory Chirikjian. *Stochastic Models, Information Theory, and Lie Groups, Volume 2: Analytic Methods and Modern Applications*. Vol. 2. Springer Science & Business Media, 2011.
- [9] Guoquan Huang. “Improving the Consistency of Nonlinear Estimators: Analysis, Algorithms, and Applications”. PhD thesis. Department of Computer Science and Engineering, University of Minnesota, 2012.
- [10] J. A. Hesch et al. “Consistency Analysis and Improvement of Vision-aided Inertial Navigation”. In: *IEEE Transactions on Robotics* 30.1 (2014), pp. 158–176. ISSN: 1941-0468. DOI: [10.1109/TRO.2013.2277549](https://doi.org/10.1109/TRO.2013.2277549).
- [11] Yulin Yang and Guoquan Huang. “Acoustic-Inertial Underwater Navigation”. In: *2017 IEEE International Conference on Robotics and Automation (ICRA)*. IEEE. 2017.